Scientific Research and Essays

Volume 10 Number 18 30 September 2015
ISSN 1992-2248

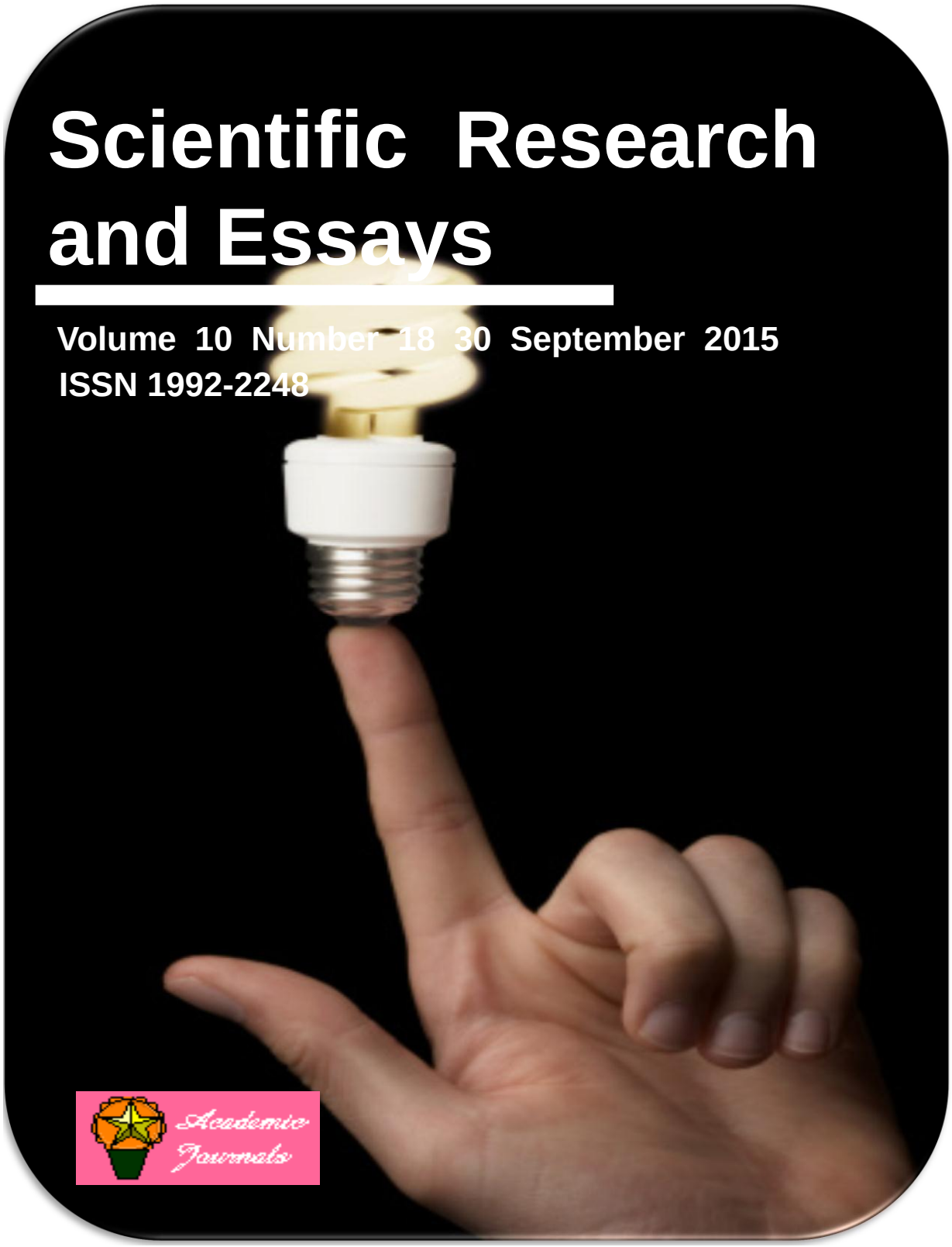

Academic Journals

ABOUT SRE

The **Scientific Research and Essays (SRE)** is published twice monthly (one volume per year) by Academic Journals.

Scientific Research and Essays (SRE) is an open access journal with the objective of publishing quality research articles in science, medicine, agriculture and engineering such as Nanotechnology, Climate Change and Global Warming, Air Pollution Management and Electronics etc. All papers published by SRE are blind peer reviewed.

Submission of Manuscript

Submit manuscripts as email attachment to the Editorial Office at sre@academicjournals.org. A manuscript number will be mailed to the corresponding author shortly after submission.

The Scientific Research and Essays will only accept manuscripts submitted as e-mail attachments.

Please read the **Instructions for Authors** before submitting your manuscript. The manuscript files should be given the last name of the first author.

Editors

Dr.NJTonukari
Editor-in-Chief
ScientificResearchandEssays
AcademicJournals
E-mail:sre.research.journal@gmail.com

Dr.M.SivakumarPh.D. (Tech).
AssociateProfessor
SchoolofChemical&EnvironmentalEngineering
FacultyofEngineeringUniversityofNottingham
JalanBroga,43500Semenyih
SelangorDarul Ehsan
Malaysia.

Prof.N.MohamedElSawiMahmoud*Departmentof Biochemistry,Facultyofscience,KingAbdulAzizuniversity,*
SaudiaArabia.

Prof.AliDelice
ScienceandMathematicsEducationDepartment,AtatürkFacultyofEducation,
MarmaraUniversity,
Turkey.

Prof.MiraGrdisa
RudjerBoskovicInstitute,Bijenickacesta54,
Croatia.

Prof.EmmanuelHalaKwon-Ndung*NasarawaStateUniversityKeffiNigeria PMB1022Keffi,*
NasarawaState.
Nigeria.

Dr.CyrusAzimi
DepartmentofGenetics,CancerResearchCenter,
CancerInstitute,TehranUniversityofMedicalSciences,KeshavarzBlvd.,
Tehran,Iran.

Dr.Gomez,NidiaNoemi
NationalUniversity ofSan Luis,
FacultyofChemistry,BiochemistryandPharmacy,
LaboratoryofMolecularBiochemistryEjercitodelosAndes950-5700SanLuis
Argentina.

Prof.M.NageebRashed
ChemistryDepartment-FacultyofScience,Aswan SouthValleyUniversity,
Egypt.

Dr.JohnW.Gichuki
KenyaMarine& FisheriesResearchInstitute,
Kenya.

Dr.WongLeongSing*Department ofCivilEngineering,CollegeofEngineering,UniversitiTenagaNational,*
Km7,JalanKajang-Puchong,
43009Kajang,SelangorDarulEhsan,Malaysia.

Prof.XianyiLI
CollegeofMathematicsandComputationalScience
ShenzhenUniversity
Guangdong,518060
P.R.China.

Prof.MevlutDogan
KocatepeUniversity,ScienceFaculty,PhysicsDept.Afyon/Turkey.
Turkey.

Prof.Kwai-LinThong*MicrobiologyDivision,InstituteofBiologicalScience,*
FacultyofScience,University ofMalaya,50603,KualaLumpur,
Malaysia.

Prof.XiaocongHe
FacultyofMechanicalandElectricalEngineering,Kunming University ofScienceandTechnology,253XueFuRoad,Kunming,
P.R.China.

Prof.SanjayMisra
DepartmentofComputerEngineering
SchoolofInformationandCommunicationTechnologyFederalUniversityofTechnology,Minna,
Nigeria.

Prof.BurtramC.FieldingPr.Sci.Nat.*DepartmentofMedicalBioSciencesUniversityoftheWesternCapePrivateBagX17*
ModderdamRoad
Bellville,7535,
SouthAfrica.

Prof.NaqibUllahKhan
DepartmentofPlantBreedingandGenetics
NWFPAgriculturalUniversityPeshawar25130,Pakistan

Editorial Board

Prof.AhmedM.Soliman
20MansourMohamedSt.,Apt51,Z amalek,Cairo, Egypt.

Prof.JuanJoséKasperZubillaga
Av.Universidad1953Ed.13depto304, MéxicoD.F.04340, México.

Prof.ChauKwok-wing
UniversityofQueenslandInstitut oMexicanodelPetroleo,EjeCentr alLazaroCardenasMexicoD.F., Mexico.

Prof. Raj Senani
Netaji Subhas Institute of Technology, AzadHind Fauj Marg, Sector3, Dwarka, New Delhi 110075, India.

Prof. RobinJ Law
CefasBurnhamLaboratory, RemembranceAvenueBurnhamonCrouch,E ssexCM08HA, UK.

Prof. V. Sundarapandian
IndianInstitute ofInformation Technologyand Management-Kerala ParkCentre, TechnoparkCampus,KariavattomP.O., Thiruvananthapuram-695581,Kerala,India.

Prof. Tzung-PeiHong
Department of Electrical Engineering, Andat the Department of Computer Science and Information Engineering NationalUniversity ofKaohsiung.

Prof.ZulfiqarAhmed
DepartmentofEarthSciences,box5070, Kfupm,dhahran-31261,SaudiArabia.

Prof. Khalifa Saif Al-Jabri
Department of Civil and Architectural Engineering College of Engineering, Sultan Qaboos University P.O.Box33,Al-Khod123,Muscat.

Prof.V.Sundarapandian
IndianInstitute ofInformationTechnology&Management-Kerala ParkCentre, Technopark,KariavattomP.O. Thiruvananthapuram-695581,KeralaIndia.

Prof.ThangaveluPerianan
DepartmentofMathematics,AditanarCollege,Ti ruchendur-628216India.

Prof.Yan-zePeng
DepartmentofMathematics, HuazhongUniversityofScience and Technology,Wuhan430074,P.R. China.

Prof.KonstantinosD.Karamanos
UniversiteLibredeBruxelles, CP231Centre ofNonlinear Phenomena AndComplexsystems, CENOLIBoulevarddeTriomphe B-1050, Brussels,Belgium.

Prof.XianyiLI
SchoolofMathematicsandPhysics,Nanhu aUniversity,HengyangCity,HunanProvinc e, P.R.China.

Dr.K.W.Chau
HongKongPolytechnicUniversity DepartmentofCivil&StructuralEngineering,Ho ngKongPolytechnicUniversity,Hunghom,Kowl oon,HongKong, China.

Dr.AmadouGaye
LPAO-SF/ESPPoBox5085Dakar-FannSENEGAL UniversityCheikhAntaDiopDakarSE NEGAL.

Prof.MasnoGinting
P2F-LIPI,Puspiptek-Serpong, 15310IndonesianInstituteofSciences, Banten-Indonesia.

Dr. Ezekiel Olukayode Idowu
Department of Agricultural Economics, Obafemi Awolowo University, Ife-Ife, Nigeria.

Fees and Charges: Authors are required to pay a $550 handling fee. Publication of an article in the Scientific Research and Essays is not contingent upon the author's ability to pay the charges. Neither is acceptance to pay the handling fee a guarantee that the paper will be accepted for publication. Authors may still request (in advance) that the editorial office waive some of the handling fee under special circumstances.

Copyright: © 2012, Academic Journals.
All rights Reserved. In accessing this journal, you agree that you will access the contents for your own personal use But not for any commercial use. Any use and or copies of this Journal in whole or in part must include the customary bibliographic citation, including author attribution, date and article title.

Submission of a Manuscript Implies: that the work described has not been published before (except in the form of an abstract or as part of a published lecture, or thesis) that it is not under consideration for publication elsewhere; that if and when the manuscript is accepted for publication, the authors agree to automatic transfer of the copyright to the publisher.

Disclaimer of Warranties

In no event shall Academic Journals be liable for any special, incidental, indirect, or consequential damages of any kind arising out of or in connection with the use of the articles or other material derived from the SRE, whether or not advised of the possibility of damage, and on any theory of liability.

This publication is provided “as is" without warranty of any kind, either expressed or implied, including, but not Limited to, the implied warranties of merchantability, fitness for a particular purpose, or non-infringement. Descriptions of, or references to, products or publications does not imply endorsement of that product or publication. While every effort is made by Academic Journals to see that no in accurate or misleading data, opinion or statements appear in this publication, they wish to make it clear that the data and opinions appearing in the articles and advertisements herein are the responsibility of the contributor or advertiser concerned. Academic Journals makes no warranty of any kind, either express or implied, regarding the quality, accuracy, availability, or validity of the data or information in this publication or of any other publication to which it may be linked.

Scientific Research and Essays

Table of Contents: Volume 10 Number 18 30 September, 2015

ARTICLES

Research Articles

academicJournals

Vol. 10(18), pp. 579-592, 30 September, 2015
DOI: 10.5897/SRE2015.6258
Article Number: 54B2BEA55372
ISSN 1992-2248
Copyright©2015
Author(s) retain the copyright of this article
http://www.academicjournals.org/SRE

Scientific Research and Essays

Full Length Research Paper

A comparison of functional properties of native Malawian cocoyam, sweetpotato and cassava starches

Davies Emmanuel Mweta[1]*, John Danwell Kalenga-Saka[2] and Maryke Labuschagne[3]

[1]Malawi University of Science and Technology, P. O. Box 5196, Limbe, Malawi.
[2]University of Malawi, Chancellor College, P. O. Box 280, Zomba, Malawi.
[3]University of the Free State, P. O. Box 339, Bloemfontein 9300, South Africa.

Received 15 May, 2015; Accepted 9 September, 2015

Cassava, cocoyam and sweetpotato constitute underexploited but yet important sources of starch for the Malawi industry. The functional properties of starches isolated from cassava, cocoyam and sweetpotato were studied and compared. Results revealed diverse functional properties among the starches from the different sources. With increasing temperature, water binding capacity, swelling power and solubility of the starches increased. Cocoyam and sweetpotato starches exhibited lower water binding capacity and swelling power, paste clarity and viscosity but higher degree of syneresis than cassava starches. Solubility was higher in cocoyam starches than sweetpotato and cassava starches. Cocoyam starches had higher gelatinization temperatures than sweet potato and cassava starches but similar transition enthalpies with cassava. Retrogradation studies by differential scanning calorimetry and turbidometry revealed higher levels of retrogradation for cocoyam and sweetpotato starches compared to cassava starches. Thus starches from sweetpotato, cocoyam and cassava would play different roles in various industrial applications.

Key words: Sweetpotato, cocoyam, cassava, starch, functional properties.

INTRODUCTION

Starch is widely used in different applications in the food and non-food industries. Its application is primarily determined by its functional properties which vary with botanical source (Wickramasinghe et al., 2009; Nwokocha et al., 2009; Yuan et al., 2007; Amani et al., 2004). The demand for starch in industries worldwide is currently being met by a restricted number of crops mainly corn, potato and wheat. Tropical root and tuber crops of which sweetpotato (*Ipomoea batatas*), cocoyam (*Colocasia esculenta*) and cassava (*Manihot esculenta*) are important representatives, remain underexploited sources of starch for the industry worldwide despite being rich in starch (Ellis et al., 1998). In Malawi, these three crops are grown mainly as subsistence crops limiting their potential contribution to the starch-based industries. Hence there is need for unveiling the characteristic properties of

*Corresponding author. E-mail: dmweta@must.ac.mw. Tel: +265 1 478 278, +265 888 364444.
Author(s) agree that this article remain permanently open access under the terms of the Creative Commons Attribution License 4.0 International License

starches from these crops in order to unravel the potential and increase the competitiveness of starches from these crops on the world markets. This study therefore, was undertaken to determine and compare the functional properties of native starches from sweetpotato, cocoyam and cassava grown in Malawi.

MATERIALS AND METHODS

Starch from 15 genotypes of sweetpotato (A45, Babache, Kakoma, Kamchiputu, Kenya, Lunyangwa, LU96/303, LU96/304, Mafutha, Mugamba, Mugande, Salera, Semusa, Tainoni and Zondeni), 7 cocoyam accessions collected from different cocoyam growing districts of Malawi (Chitipa, Mzimba (Mzuzu), Nkhotakota, Machinga, Mulanje, Thyolo and Zomba) and five genotypes of cassava (Gomani, Maunjili, Mbundumali, Mkondezi and Sauti) were used for this study.

Starch isolation

Starch was isolated from the fresh tubers as follows: Fresh tuberous roots were washed, peeled, washed again and chopped to about 1 cm^3 cubes. About 500 g of the chopped tubers were transferred into a heavy duty blender (Warring Commercial, model CBCSA 33BL34), 1 L of water added, and pulverized at a high speed for 5 min. The suspension was then filtered using a 250 µm sieve. The filtrate was allowed to stand for four hours to facilitate starch sedimentation and the top liquid was decanted and discarded. The sediment was resuspended in 1 L of water and the whole process was repeated three times. The sediment was then washed and dried in an air-dried for 48 h. The dried starch was ground and stored in polyethylene bottles prior to analysis.

Water binding capacity (WBC)

Water binding capacity (WBC) of the starches was determined using 2.5% starch suspensions at three temperatures; 50, 70 and 90°C. Dried starch samples of 0.125 g were weighed in triplicates into pre-weighed centrifuge tubes and 5 ml of distilled water added. The samples were heated at each of the above temperature for 1 h with constant shaking and thereafter centrifuged for 15 min at 1500 × *g*. The free water was decanted and the tubes allowed draining off for 10 min at a 45° angle. Subsequently the sample tubes were weighed, and the gain in weight used to calculate the water binding capacity. Water binding capacity was calculated using the following equation(Mishra and Rai, 2006):

WBC (g H_2O g^{-1}) = (Mass of wet starch - Mass of dry starch)/ Mass of dry starch.

Swelling power and solubility

Swelling and solubility of the starches was determined in triplicates as follows: Dried starch samples (0.100 g) were mixed with 5 ml of distilled in 10 ml centrifuge tubes, heated for 1 h at 50, 70 or 90°C while shaking every 5 min. The slurry was centrifuged for 30 min at 1500 × *g*, and the weight of the sediment in grams (B) determined (Kojima et al., 2006). The supernatant (A) was diluted with water until the total volume was 10 mL, and the amount of starch in it was determined by anthrone-sulphuric acid method (Brook et al., 1986). The solubility and the swelling power were calculated using the following equations, where (S) is the sample weight in grams.

Solubility (%) = (100 x A)/S
Swelling power (g g^{-1}) = B/(S-A)

Clarity and stability of starch pastes

Clarity and stability of the starch pastes was determined by the method of Craig et al. (1986) as follows: a 1% aqueous suspension of starch was made by adding 10 mL of distilled water to exactly 0.1 g of starch (dry basis) in a centrifuge tube with screw caps and vortex mixed. The suspension was heated in a boiling water bath for 30 min with constant stirring every 5 min and thereafter cooled to room temperature for 1 h. The percentage transmittance (%T) was measured at 650 nm against a water blank on a spectrophotometer (Spectronic Unicam, Heλios, Cambridge, United Kingdom).

The stability of the starch pastes was determined by placing triplicate starch paste samples prepared above in disposable cuvettes and stored for 5 days at 4°C in a refrigerator. Turbidity was determined every 24 h by measuring absorbance at 640 nm against a water blank (Sandhu and Singh, 2007).

Syneresis

A 5% aqueous starch suspension was made by adding 5 ml of distilled water to 0.25 g (db) in screw-capped centrifuge tube. The suspension was heated in a boiling water bath for 30 min with constant stirring and then cooled rapidly to room temperature on ice bath. After cooling, the tubes with the starch pastes were reweighed to determine the amount of starch paste and then placed in a still-air freezer at -20°C for 48 h. After the freezing period, the samples were placed in a 40°C water bath for 1.5 h to thaw and equilibrate. Syneresis was measured in triplicate as % amount of water released after centrifuging at 1500 x g for 30 min (Singh et al., 2004).

Viscosity

The viscosity of the starch pastes was determined using a Brookfield Digital Viscometer model RTDV II (Brookfield Engineering Laboratories Inc, Stoughton MA 02072, USA) with modifications (ISI, 2002). A 10% starch suspension was prepared in duplicate for each sample by weighing 10 g of dried starch samples into a 600 mL beaker and adding distilled water to bring to the total weight of starch and water to 500 g. The starch suspension was heated in a water bath at 95°C for 30 min with constant stirring. The resultant gelatinized starch was weighed and water added to replace the evaporated water until the gross weight of 500 g. The starch gel was cooled to 50°C in a water bath set at 50°C while stirring and viscosity measured in centipoises (cps) with spindle no. 2 at 100 rpm.

Thermal properties

Thermal properties of raw starches and retrograded were obtained using differential scanning calorimetry (DSC 822e, Mettler, Toledo, Switzerland). Starch samples were prepared by mixing dried starch with distilled water in a ratio of 1:3. Exactly 3.0 mg, in triplicates, of dried starch were weighed into DSC aluminium pans and distilled water added using a transfer pipette to make a starch: water ratio of 1:3. The pans were hermetically sealed and samples were left to stand for 1 h at room temperature for moisture equilibration. The sealed pans were heated from 20 to 95°C under nitrogen gas at a heating rate of 10°C/min to gelatinize the starch samples. From the

DSC thermograms, onset temperature (T_o), peak temperature (T_p), conclusion temperature (Tc) and enthalpy of gelatinization (ΔH_G) were determined using instruments software (STARe SW 9.00). Temperature range and peak height index (PHI) were also calculated as T_c - T_o and as the ratio $\Delta H_G/(T_p-T_o)$ respectively (Peroni et al., 2006)

The gelatinized samples from the gelatinization studies described above were stored at 4°C (refrigerator) for a period of 7 days, equilibrated at room temperature for 2 h, and then rescanned in the DSC from 20 to 95°C at 10°C/min to measure the retrogradation transition temperatures and enthalpy. The degree of retrogradation was determined as the ratio of enthalpy change of retrograded starch to enthalpy change of gelatinized starch (Gunaratne and Hoover, 2002).

Data analysis

Data obtained was subjected to analysis of variance (ANOV A) using Statistix 8 for Windows (Analytical Software Tallahassee, USA). Principal component analysis (PCA) was also performed on the determined functional properties of the starches using NCSS 2004 (Number Cruncher Statistical systems, Kaysville, Utah, USA) in order to identify the main variables that described the similarities and differences between starches and also to find the relationships between the measured properties. Pearson correlation coefficients for relationships between various functional properties were also calculated.

RESULTS AND DISCUSSION

Water binding capacity (WBC)

The water binding capacity of the starches significantly increased with temperature with high increases observed between 50 to 70°C for all starches (Table 1). Generally, cassava starches exhibited significant higher WBC values than sweetpotato and cocoyam starches at all temperatures. Between 50 to 90°C, WBC values ranged from 1.49 to 38.70, 1.28 to 28.31 and 1.47 to 24.71 g H_2O g^{-1}, for cassava, cocoyam and sweetpotato starches, respectively. Variations in WBC within the same botanical source were also observed. Among the cassava genotypes, starch from Sauti displayed the highest WBC at the three temperatures whilst among the cocoyam accessions, starch from Chitipa accession exhibited higher WBC values at 70 and 90°C. No consistent trends were observed among sweetpotato starches. Water binding is a measure of the amount of water that starch granules are able to hold and depends on the capacity of starch molecules to hold water through hydrogen bonding. These observed differences in WBC therefore, indicate the differences in the intensity of the hydrogen bonds forms and the degree of availability of water binding sites among the starches (Hoover and Sosulski, 1986). This ability to hold water is a desirable characteristic in the food industry for consistency of food products. Therefore cassava starches are better suited for the food industry as gelling agents than cocoyam and sweetpotato starches (Gbadamosi et al., 2013). They could also be used in frozen food products as stabilisers and emulsifiers as starches with high WBC usually bind more water preventing syneresis (Otegbayo et al., 2013).

Swelling power and solubility patterns

The swelling power of the starches increased with increasing temperature from 50 to 90°C. This is probably due to the breaking of intermolecular hydrogen bond in the amorphous areas (De la Torre-Gutiérrez et al., 2008). There were significant variations in swelling power among the starches. Generally, the cocoyam and sweetpotato starches exhibited lower swelling power than cassava starches at all temperatures; cassava starches exhibited the highest swelling power (Table 2). The swelling power of the cocoyam starches ranged from 2.29 to 34.10 g g^{-1} from 50 to 90°C while that of sweetpotato starches ranged from 2.49 to 28.22 g g^{-1} from 50 to 90°C. Swelling power of cassava starches ranged 2.50 to 43.81 g g^{-1} from 50 to 90°C. These results agree with those reported by Wickramasinghe et al. (2009). They reported higher swelling power for cassava starches than taro (*Colocasia esculenta*) and sweetpotato starches. Gbadamosi et al. (2013) also reported higher swelling power for cassava starches than cocoyam starches. However they reported lower values of swelling power for cassava and cocoyam starches than the ones observed in this study. Bentacur-Ancona et al. (2001) reported higher swelling power values (58.8 g g^{-1}) for cassava values than the ones obtained in this study.

Solubility of the starches increased with increasing temperature (Table 3). This is because an increase in temperature increases the mobility of starch granules thereby facilitating dispersion of starch molecules in water. The heated and swollen starch granules consequently for allow amylose exudation (Adebowale et al., 2002). Cocoyam starches generally displayed higher solubility than cassava and sweetpotato starches, and sweetpotato starches displayed the lowest solubility. Solubility of cocoyam, cassava and sweetpotato starches ranged from 0.22 to 15.68%, 0.36 to 10.11% and 0.41 to 9.43% from 50 to 90°C, respectively. These results contrast those of Gbadamosi et al. (2013) who reported higher solubility for cassava starches that cocoyam starches.

Both swelling power and solubility provide evidence of the magnitude of interactions between starch chains within the amorphous and crystalline regions. Swelling power is influenced by a strong bonded micellar network and amylopectin molecular structure decreasing with increasing crystallite formation by the association between long amylopectin chains (Srichuwong et al., 2005; Gujska et al., 1994; Sasaki and Masuki, 1998). Thus, the differences in the extent of swelling observed in this study indicate differences in structures among the starches. The differences in solubility of the starches could largely be due to granular and molecular structural

Table 1. Water binding capacity of the cocoyam, sweetpotato and cassava starches.

Botanical source	Accession/genotype	Water binding capacity [g H_2O g^{-1} starch]		
		50°C	70°C	90°C
Cocoyam	Chitipa	1.50^{ij}	**13.42^{fgh}**	**28.31^{c}**
	Machinga	1.31^{k}	6.07^{m}	24.35^{f}
	Mulanje	1.39^{jk}	6.31^{m}	22.04^{h}
	Mzuzu	1.28^{k}	10.91^{j}	22.69^{gh}
	Nkhotakota	1.48^{ij}	2.35^{n}	25.72^{d}
	Thyolo	1.49^{ij}	10.98^{j}	25.65^{de}
	Zomba	1.60^{fghi}	6.04^{m}	22.60^{gh}
	Mean	1.44±0.13	8.01±3.68	24.48±2.20
Sweetpotato	A45	1.80^{cd}	8.22^{l}	20.58^{i}
	Babache	1.66^{efg}	8.09^{l}	20.05^{ijkl}
	Kakoma	1.83^{cd}	11.96^{i}	19.37^{kl}
	Kamchiputu	1.71^{def}	13.67^{f}	19.96^{ijkl}
	Kenya	1.48^{ij}	13.46^{fg}	19.54^{jkl}
	Lunyangwa	1.51^{hij}	13.74^{f}	17.70^{m}
	LU96/303	1.57^{ghi}	11.90^{i}	17.84^{m}
	LU96/304	1.50^{ij}	13.07^{fgh}	19.28^{l}
	Mafutha	1.60^{fghi}	13.09^{fgh}	19.96^{ijkl}
	Mugamba	1.63^{fgh}	14.84^{e}	20.31^{ijk}
	Mugande	1.86^{c}	12.75^{h}	20.17^{ijkl}
	Salera	1.47^{ij}	11.14^{j}	23.13^{g}
	Semusa	1.52^{hij}	9.53^{k}	18.14^{m}
	Tainoni	1.73^{def}	12.84^{gh}	24.72^{ef}
	Zondeni	1.77^{cde}	10.01^{k}	20.49^{ij}
	Mean	1.64±0.15	11.88±2.05	20.08±1.86
Cassava	Gomani	1.82^{cd}	15.43^{de}	34.39^{b}
	Maunjili	2.22^{b}	17.53^{a}	34.07^{b}
	Mbundumali	1.49^{ij}	15.88^{cd}	38.30^{a}
	Mkondezi	1.79^{cde}	16.18^{bc}	38.70^{a}
	Sauti	**3.40^{a}**	**16.74^{b}**	**38.46^{a}**
	Mean	2.14±0.70	16.35±0.80	36.78±2.20

Means followed by the same letter within the same column are not significantly different from each other (p≤0.05); Means for botanical source expressed as mean ± standard deviation.

Table 2. Swelling power of the cocoyam, sweetpotato and cassava starches.

Botanical source	Genotype/ accession	Swelling power (g g^{-1} starch)		
		50°C	70°C	90°C
Cocoyam	Chitipa	2.50^{jklm}	16.08^{ef}	34.10^{c}
	Machinga	2.32^{n}	7.54^{q}	29.39^{de}
	Mulanje	2.40^{mn}	7.74^{q}	26.63^{gh}
	Mzuzu	2.29^{n}	12.79^{mn}	27.57^{fg}
	Nkhotakota	2.50^{klm}	3.36^{r}	28.16^{ef}
	Thyolo	2.51^{jklm}	13.03^{lmn}	29.95^{d}
	Zomba	2.61^{ghijk}	7.44^{q}	28.52^{ef}
	Mean	2.44±0.13	9.71±4.18	29.19±2.46
Sweetpotato	A45	2.70^{efg}	9.50^{p}	23.12^{ij}
	Babache	2.67^{fgh}	9.35^{p}	22.42^{jk}

Table 2. Contd.

	Kakoma	2.85^{c}	13.72^{kl}	21.77^{kl}
	Kamchiputu	2.73^{def}	15.63^{fg}	22.89^{ijk}
	Kenya	2.49^{lm}	15.17^{ghi}	22.13^{jk}
	Lunyangwa	2.52^{jkl}	15.46^{fgh}	19.96^{m}
	LU96/303	2.58^{hijkl}	13.45^{lm}	20.67^{lm}
	LU96/304	2.51^{jklm}	14.73^{hij}	21.61^{kl}
	Mafutha	2.62^{fghij}	14.88^{ghij}	22.61^{ijk}
	Mugamba	2.64^{fghi}	16.83^{de}	23.22^{ij}
	Mugande	2.89^{c}	14.35^{jk}	22.73^{ijk}
	Salera	2.49^{lm}	12.58^{n}	25.99^{h}
	Semusa	2.54^{ijkl}	11.34^{o}	20.81^{lm}
	Tainoni	2.66^{fghi}	14.48^{ijk}	28.22^{ef}
	Zondeni	2.79^{cde}	11.39^{o}	23.81^{i}
	Mean	2.64±0.14	13.52±2.23	22.80±2.11
Cassava	Gomani	2.84^{cd}	17.28^{cd}	37.36^{b}
	Maunjili	3.24^{b}	19.43^{a}	38.48^{b}
	Mbundumali	2.50^{jklm}	17.96^{bc}	43.44^{a}
	Mkondezi	2.79^{cde}	18.32^{b}	43.81^{a}
	Sauti	4.44^{a}	18.76^{ab}	43.39^{a}
	Mean	3.16±0.71	18.35±0.84	41.30±2.95

Means followed by the same letter within the same column are not significantly different from each other (p≤ 0.05); Means for botanical source expressed as mean ± standard deviation.

differences among the starches (Bello-Pérez et al., 2000; Tian and Rickard, 1991). The high swelling power of cassava starches coupled with high water binding capacity makes them ideal for their exploitation in the food industry where they could be utilised as thickeners.

Paste clarity and stability

Generally, cassava starches had higher paste clarity (33.8±6.0%) than sweetpotato (16.1±2.5%) and cocoyam (15.9±3.5%) starches (Table 4). The paste clarity of the cocoyam and sweetpotato starches was comparable. Maunjili starch exhibited the highest paste clarity among the cassava starches whilst Mugande, Semusa and Kenya starches displayed higher paste clarity among sweetpotato starches. Chitipa and Mzuzu starch provided the highest clarity among the cocoyam starches. Nwokocha et al. (2009) also reported higher paste clarity for cassava starches than cocoyam starches. Amylose and phosphorus contents are known to influence clarity of starch pastes. High amylose content may result in more opaque starch pastes (Schmitz et al., 2006), while presence of high amounts of phosphate groups tends to increase starch paste clarity (Jane et al., 1996). Lower paste clarity of cocoyam and sweetpotato starches compared to cassava starches suggests the presence of amylose molecules of high susceptibility to retrogradation (Craig et al., 1989).

For the five days of refrigerated storage, opacity of the cocoyam, sweetpotato and cassava starch paste increased (Table 4). Greater increases in opacity were observed in cocoyam and sweetpotato starches than in cassava starches indicating higher retrogradation tendencies for cocoyam and sweetpotato starches than cassava starches. Turbidity development during storage arises from interaction of several factors, such as granule swelling, granule remnants, leached amylose and amylopectin, amylose and amylopectin chain length, intra or interbonding, and lipid (Jacobson et al., 1997). The high retrogradation tendencies displayed by cocoyam and sweetpotato starches in this study suggest that these starches are not ideal for food products that require freezing and thawing. However low retrogradation tendencies displayed by cassava starches makes them ideal for such application.

Paste viscosity and Syneresis

Generally cassava starches exhibited higher paste viscosity than sweetpotato and cocoyam staches (Table 5). The paste viscosity ranged from 10140 to 14033 cps, 5333 to 8733 and 6067 cps 12733 cps for cassava, cocoyam and sweetpotato starches, respectively.Thus cassava starches displayed the highest tendency to form viscous pastes than cocoyam and sweetpotato starches. Gbadamosi et al. (2013) reported the contrary; they found

Table 3. Solubility of the cocoyam, sweetpotato and cassava starches

Botanical source	Genotype/ accession	Solubility (%)		
		50°C	70°C	90°C
Cocoyam	Chitipa	0.22^{o}	10.30^{a}	15.68^{a}
	Machinga	0.31^{mn}	6.19^{d}	14.32^{b}
	Mulanje	0.30^{n}	6.11^{d}	12.48^{c}
	Mzuzu	0.55^{defgh}	6.85^{c}	10.66^{e}
	Nkhotakota	0.51^{fghij}	4.46^{jkl}	7.45^{l}
	Thyolo	0.54^{efghi}	8.05^{b}	11.69^{d}
	Zomba	0.58^{abcde}	5.91^{de}	14.08^{b}
	Mean	0.43±0.15	6.84±1.79	12.34±2.61
Sweet potato	A45	0.41^{kl}	2.93^{m}	6.43^{no}
	Babache	0.47^{jk}	2.86^{m}	5.95^{qr}
	Kakoma	0.54^{efghi}	5.55^{ef}	6.70^{mn}
	Kamchiputu	0.58^{abcde}	6.13^{d}	9.15^{hi}
	Kenya	0.52^{efghij}	4.98^{gh}	7.98^{k}
	Lunyangwa	0.50^{ghij}	4.20^{kl}	6.31^{op}
	LU96/303	0.53^{efghij}	4.07^{l}	6.06^{pq}
	LU96/304	0.61^{abcd}	4.53^{ijk}	5.72^{r}
	Mafutha	0.56^{cdefg}	5.29^{fg}	7.29^{l}
	Mugamba	0.48^{ij}	5.91^{de}	8.48^{j}
	Mugande	0.63^{ab}	4.14^{l}	6.69^{mn}
	Salera	0.50^{hij}	4.07^{l}	6.98^{m}
	Semusa	0.57^{bcdef}	3.13^{m}	7.52^{l}
	Tainoni	0.64^{a}	4.46^{jkl}	8.23^{jk}
	Zondeni	0.58^{abcde}	2.93^{m}	9.43^{gh}
	Mean	0.54±0.07	4.35±1.07	7.26±1.15
Cassava	Gomani	0.62^{abc}	4.90^{hi}	10.11^{f}
	Maunjili	0.48^{ij}	4.61^{hij}	8.86^{i}
	Mbundumali	0.36^{lm}	6.30^{d}	9.54^{g}
	Mkondezi	0.38^{lm}	6.27^{d}	9.46^{g}
	Sauti	0.56^{cdefg}	5.39^{f}	9.06^{i}
	Mean	0.48±0.11	5.49±0.74	9.41±0.45

Means followed by the same letter within the same column are not significantly different from each other (p≤ 0.05); Means for botanical source expressed as mean ± standard deviation.

that cocoyam starches had the greatest tendency to form viscous pastes. Since starches are used in industries to impart viscosity, the use of cassava, sweetpotato or cocoyam starches will be determined by the desired viscosity of the end product. Cassava starches could be explored in the adhesive industries where high viscosity provides and appreciable binding capacity.

Syneresis is the exeudation of water from frozen gels during retrogradation process and is therefore an indication of retrogradation tendencies of the starch pastes (Otegbayo et al., 2013). The degree of syneresis ranged from 28.9 to 49.2%, 11.5 to 36.7% for cocoyam and sweetpotato starches respectively, and was 0% and for cassava starches (Table 5). Thus cassava starches were more stable to freeze-thawing than cocoyam and sweetpotato starch. Cassava starch could therefore be better suited for use in frozen products than cocoyam and sweetpotato starches (Vaclavik and Christian, 2014). Higher tendencies to lose water for sweetpotato and cocoyam starches indicate that they will have limited application in frozen food products.

Gelatinization

The gelatinization temperatures ranged from 69.4-81.4, 68.5-79.2 and 60.1-76.8°C for cocoyam, sweetpotato and cassava starches, respectively (Table 6). Generally, cocoyam starch exhibited higher onset, peak, and conclusion temperatures than sweetpotato and cassava

Table 4. Clarity and stability of the starch pastes.

Botanical source	Genotype/ accession	Paste clarity and stability at 4°C (%T)				
		Day 1	Day 2	Day 3	Day 4	Day 5
Cocoyam	Chitipa	20.4^{e}	10.0^{ef}	8.4^{ghi}	7.6^{fg}	7.0^{ef}
	Machinga	13.6^{lm}	5.9^{klmn}	4.8^{no}	4.1^{mno}	2.8^{l}
	Mulanje	16.8^{ghij}	7.6^{hijk}	6.2^{kl}	4.9^{klm}	4.2^{jk}
	Mzuzu	19.8^{ef}	10.5^{e}	9.2^{f}	8.2^{f}	7.4^{ef}
	Nkhotakota	12.6^{mn}	5.5^{lmn}	3.9^{pq}	3.0^{p}	2.5^{l}
	Thyolo	10.9^{n}	4.7^{mn}	4.1^{0pq}	3.5^{op}	2.9^{l}
	Zomba	17.1^{hij}	9.1^{efghi}	6.6^{k}	5.1^{jkl}	4.5^{ij}
	Mean	15.9±3.5	7.6±2.2	6.2±2.0	5.2±1.9	4.5±1.9
Sweetpotato	A45	10.9^{n}	4.5^{n}	3.6^{q}	2.9^{p}	2.5^{l}
	Babache	15.8^{ijk}	7.5^{hijk}	6.6^{k}	5.7^{ij}	5.1^{hij}
	Kakoma	16.2^{hijk}	8.6^{fghij}	6.5^{kl}	5.9^{i}	5.5^{ghi}
	Kamchiputu	17.6^{ghi}	8.0^{ghij}	5.2^{mn}	4.8^{klm}	4.6^{hij}
	Kenya	18.0^{fgh}	9.4^{efgh}	8.8^{fgh}	8.2^{f}	7.8^{e}
	Lunyangwa	15.8^{ijk}	8.1^{fghij}	6.6^{k}	6.1^{i}	5.6^{gh}
	LU96/303	16.4^{hijk}	9.2^{efghi}	8.1^{hij}	7.0^{g}	6.5^{fg}
	LU96/304	15.4^{jkl}	8.0^{ghij}	7.6^{j}	6.2^{hi}	5.5^{ghi}
	Mafutha	17.6^{ghi}	8.5^{fghij}	7.7^{ij}	7.0^{gh}	6.6^{fg}
	Mugamba	17.7^{ghi}	9.8^{efg}	8.9^{fg}	8.1^{f}	7.7^{e}
	Mugande	18.7^{efg}	9.6^{efg}	8.7^{fgh}	7.6^{fg}	7.1^{ef}
	Salera	15.2^{jkl}	7.3^{ijkl}	6.5^{kl}	5.6^{ijk}	5.0^{hij}
	Semusa	18.7^{efg}	10.5^{e}	9.2^{f}	8.0^{f}	7.1^{ef}
	Tainoni	14.4^{klm}	6.6^{jklm}	5.8^{lm}	4.7^{lmn}	4.1^{jk}
	Zondeni	12.9^{mn}	5.2^{mn}	4.6^{nop}	3.9^{no}	3.3^{kl}
	Mean	16.1±2.5	8.0±2.1	7.0±1.7	6.1±1.6	5.6±1.5
Cassava	Gomani	23.5^{d}	20.5^{d}	18.4^{e}	18.0^{e}	16.8^{d}
	Maunjili	40.9^{a}	35.9^{a}	34.0^{a}	32.8^{a}	33.0^{a}
	Mbundumali	33.1^{c}	28.6^{c}	27.2^{b}	25.4^{d}	23.6^{c}
	Mkondezi	36.6^{b}	33.0^{b}	31.5^{b}	29.0^{b}	27.1^{b}
	Sauti	35.0^{bc}	31.8^{b}	30.5^{c}	27.6^{c}	26.4^{b}
	Mean	33.8±6.0	30.0±5.5	28.3±5.7	26.6±5.1	25.4±5.6

Means followed by the same letter within the same column are not significantly different from each other (p≤ 0.05).

starches. Thus cassava starches gelatinised at lower temperature range than cocoyam and sweetpotato starches. The low gelatinisation temperatures for cassava starches suggest they could be used in the adhesive industries as minimal heat energy would be required when producing hot-melt glues. The enthalpy of gelatinisation ranged from 13.1-15.1, 8.3-14.7 and 10.5-12.9 J/g for cassava, cocoyam and sweetpotato starches, respectively. On average, enthalpies of gelatinisation for cocoyam and cassava starches were comparable but higher than those of sweetpotato starches. These results are in agreement with those reported by Nwokocha et al. (2009). They reported lower gelatinisation temperature range for cassava starches (60.11- 72.67°C) than cocoyam starches (72.96- 80.25°C) however the gelatinisation enthalpy was higher in cocoyam starches than cassava starches. Pérez et al. (2005) also reported higher enthalpy of gelatinisation for cocoyam starches than cassava starches. During gelatinisation, there is loss of molecular order within starch granule and therefore the gelatinisation enthalpy gives an overall measure of degree of organisation (crystallinity). Thus the higher gelatinisation enthalpy values for cassava and cocoyam starches suggest a more orderly arrangement of starch molecules. Therefore there is lower degree of organisation in sweetpotato starches leading to lower enthalpies of gelatinisation (Singh et al., 2006).

Temperature range values of the starches ranged from 16.7±1.8, 12.0±2.5 and 10.7±1.2°C for cassava, cocoyam and sweetpotato starches, respectively. Cassava starches exhibited a higher temperature range than that of cocoyam and sweetpotato starches. The peak height

Table 5. Viscosity and degree of syneresis of the starch pastes.

Botanical source	Genotype/ accession	Syneresis [%]	Viscosity [cps]
Cocoyam	Chitipa	46.5^{a}	5640^{nop}
	Machinga	49.2^{a}	5453^{op}
	Mulanje	47.1^{a}	5733^{nop}
	Mzuzu	47.2^{a}	8733^{hij}
	Nkhotakota	28.9^{cde}	7067^{kl}
	Thyolo	32.9^{bc}	5333^{p}
	Zomba	32.9^{bc}	6240^{mno}
	Mean	40.7±8.6	6314±1251
Sweetpotato	A45	26.4^{de}	8160^{j}
	Babache	24.5^{e}	7320^{k}
	Kakoma	32.3^{cd}	6307^{lmn}
	Kamchiputu	14.4^{fg}	6560^{klm}
	Kenya	11.5^{g}	9800^{efg}
	Lunyangwa	18.0^{f}	9053^{ghi}
	LU96/303	33.8^{bc}	11700^{c}
	LU96/304	30.0^{cd}	9080^{ghi}
	Mafutha	26.8^{de}	9507^{fgh}
	Mugamba	32.8^{bc}	10373de
	Mugande	36.4^{b}	10633^{d}
	Salera	36.3^{b}	8547^{ij}
	Semusa	29.9^{cd}	12733^{b}
	Tainoni	33.0^{bc}	8600^{ij}
	Zondeni	36.7^{b}	6067^{mnop}
	Mean	28.1±8.3	8963±1927
Cassava	Gomani	0.0^{h}	13000^{b}
	Maunjili	0.0^{h}	10140^{def}
	Mbundumali	0.0^{h}	12267^{bc}
	Mkondezi	0.0^{h}	14033^{a}
	Sauti	0.0^{h}	11733^{c}
	Mean	0.00±0.0	12235±1393

Means followed by the same letter within the same column are not significantly different from each other ($p \leq 0.05$).

Table 6. Thermal properties: onset (T_o), peak (T_p) and conclusion (T_c) temperatures, temperature range (R), peak height index (PHI) and transition energy (ΔH_G) of the native starches.

Botanical source	Genotype/ accession	T_o [°C]	T_p [°C]	T_c [°C]	R [°C]	PHI	ΔH_G [J/g]
Cocoyam	Chitipa	61.8^{k}	69.4^{l}	78.6^{hi}	16.8^{b}	2.1^{n}	14.2^{bcd}
	Machinga	71.4^{b}	76.7^{b}	82.4^{bc}	11.1^{fg}	2.4^{jk}	11.4^{hijk}
	Mulanje	70.2^{c}	75.7^{c}	82.6^{b}	12.5^{e}	2.6^{def}	14.0^{bcd}
	Mzuzu	68.2^{gh}	73.1^{ghi}	79.2^{efgh}	11.0^{fgh}	1.7^{o}	8.3^{n}
	Nkhotakota	75.6^{a}	78.7^{a}	83.7^{a}	8.1^{m}	4.8^{a}	14.7^{ab}
	Thyolo	67.8^{h}	73.3^{g}	80.9^{cd}	13.1^{e}	2.7^{de}	14.6^{abc}
	Zomba	71.3^{b}	76.4^{b}	82.5^{b}	11.2^{fg}	2.7^{de}	13.8^{cde}
	Mean	69.4±4.0	74.8±2.9	81.4±1.8	12.0±2.5	2.7±1.0	13.4±2.1
Sweetpotato	A45	69.8^{cd}	74.9^{de}	81.4^{c}	11.6^{f}	2.5^{ghi}	12.91^{fghi}
	Babache	69.8^{cd}	74.6^{e}	80.6^{d}	10.8^{ghi}	2.6^{def}	12.4^{ghijk}
	Kakoma	68.0^{h}	73.0^{hi}	78.6^{hi}	10.6^{ghi}	2.0^{n}	10.5^{m}
	Kamchiputu	64.3^{j}	70.9^{k}	78.9^{ghi}	14.5^{d}	1.8^{o}	11.6^{kl}

Table 6. Contd.

	Kenya	68.2^{gh}	73.1^{ghi}	79.0^{ghi}	10.8^{ghij}	2.5^{efg}	12.5^{abcd}
	LU96/303	70.9^{b}	75.1^{d}	80.7^{d}	9.7^{kl}	3.5^{b}	14.0^{bcde}
	LU96/304	68.7^{ef}	73.4^{fg}	79.2^{fgh}	10.4^{hij}	2.5^{hij}	11.7^{kl}
	Lunyangwa	68.8^{ef}	73.3^{gh}	78.6^{ghi}	9.9^{jkl}	2.5^{ijk}	11.1^{lm}
	Mafutha	67.9^{h}	72.8^{i}	78.5^{i}	10.4^{ghi}	2.5^{ijk}	12.1^{ijk}
	Mugamba	68.5^{fg}	72.9^{i}	78.8^{ghi}	10.3^{ijk}	2.8^{d}	12.0^{jk}
	Mugande	69.1^{e}	73.7^{f}	79.5^{ef}	10.4^{hij}	2.7^{de}	12.2^{hijk}
	Salera	68.6^{fg}	73.4^{fg}	79.7^{e}	11.1^{fg}	2.5^{ijk}	12.0^{jk}
	Semusa	69.7^{d}	73.2^{gh}	79.2^{efg}	9.5^{l}	3.2^{c}	12.9^{fgh}
	Tainoni	68.0^{h}	72.0^{j}	77.5^{j}	9.5^{l}	3.3^{c}	12.6^{ghij}
	Zondeni	66.8^{i}	71.8^{j}	77.8^{j}	11.0^{fgh}	2.3^{kl}	11.6^{kl}
	Mean	68.5±1.5	73.2±1.1	79.2±1.0	10.7±1.2	2.6±0.4	12.3±1.1
Cassava	Gomani	60.8^{l}	65.6^{o}	76.9^{k}	16.1^{c}	3.1^{c}	14.0^{bcd}
	Maunjili	58.2^{o}	67.4^{n}	77.5^{j}	19.3^{a}	1.6^{o}	15.1^{a}
	Mbundumali	62.1^{k}	68.6^{m}	76.2^{l}	14.1^{d}	2.2^{lm}	13.4^{def}
	Mkondezi	60.2^{m}	65.7^{o}	76.8^{k}	16.6^{bc}	2.5^{fgh}	13.1^{efg}
	Sauti	59.1^{n}	65.4^{o}	76.4^{kl}	17.3^{b}	2.1^{mn}	14.1^{bcd}
	Mean	60.1±1.4	66.5±1.3	76.8±0.6	16.7±1.8	2.3±0.5	14.0±0.8

Means followed by the same letter within the same column are not significantly different from each other ($p \leq 0.05$); Mean for botanical source are expressed as mean ±SD.

index values of the cassava, sweetpotato and cocoyam starches fell within the same range. The peak height index values ranged from 1.6-3.1, 1.8-3.5 and 1.7-4.8 for cassava, sweetpotato and cocoyam starches. However, significant ($p<0.001$) variations in PHI values were observed within starches from different sweetpotato and cassava genotypes, and cocoyam accessions. Temperature range of gelatinization and PHI are indicative of the distribution of starch granules; the more heterogeneous the granules, the broader the temperature range and the lower the PHI (Sandhu et al., 2005; Karim et al., 2000). Higher amylopectin content can also lead to the narrowing of temperature range of gelatinization (Krueger et al., 1987). Thus, the differences in gelatinization temperature range and PHI of cassava, sweetpotato and cocoyam starches indicate the differences in heterogeneity and amylose/amylopectin ratio.

Retrogradation

Retrograded starches displayed lower gelatinization temperatures and smaller enthalpies (Table 7) than raw starches indicating weaker crystallinity (Sasaki, 2005). Enthalpy of retrogradation was significantly higher for cocoyam starches than both sweetpotato and cassava starches resulting in higher levels of retrogradation. Cocoyam starches exhibited higher degree of retrogradation than sweetpotato and cassava starches indicating rapid retrogradation for cocoyam starches. Higher retrogradation tendencies are attributed to crystallization involving small amylose molecules and long chain amylopectin (Peroni et al., 2006; Gudmundsson, 1994) whereas lower degree of retrogradation is attributed to higher content of short branches of amylopectin chains and long amylose molecules (Spence and Jane, 1999). The greater degree of retrogradation in cocoyam starches could therefore be attributed to higher contents of short amylopectin branches (Shi and Srib, 1992). Thus, the differences in the retrogradation tendencies of the starches confirm composition and structural differences exist among the starches from the three crops.

Principal component analysis (PCA)

The results of PCA are presented in Tables 8 and 9 and Figures 1 and 2. The first three principal components explained 85% of the total variability. Principal components 1, 2, and 3 accounted for 63.4, 13.6, and 8.3% of the variability, respectively.

Principal component 1 separated mostly cocoyam starches (Nkhotakota, Machinga, Mulanje and Zomba) from cassava starches (Sauti, Maunjili, Mkondezi, Gomani and Mbundumali) whereas component 2 separated the cocoyam and cassava starches from most of the sweetpotato starches (Figure 1). The factor loading revealed that principal component 1 contrasted cassava starches with cocoyam starches with respect to paste clarity, viscosity, water binding capacity and swelling

Table 7. Thermal properties of the retrograded starches: onset (T_o), peak (T_p) and conclusion (T_c) temperatures, temperature range (R), and transition energy (ΔH_G).

Botanical source	Accession/genotype	T_o (°C)	T_p (°C)	T_c (°C)	R (°C)	ΔH_G (J/g)	Retrog. (%)
Cocoyam	Chitipa	45.9^{m}	56.1^{p}	62.5^{j}	16.6^{ab}	3.5^{hij}	23.4^{l}
	Machinga	49.7^{kl}	58.6^{n}	65.2^{h}	15.5^{def}	5.0^{b}	41.6^{b}
	Mulanje	51.2^{j}	59.3^{jkl}	66.2^{def}	15.0^{defg}	4.4^{cde}	31.2^{efg}
	Mzuzu	52.0^{fgh}	59.0^{m}	65.3^{gh}	13.3^{j}	3.8^{g}	45.3^{a}
	Nkhotakota	51.8^{fghi}	59.7^{hi}	66.0^{defg}	14.2^{ghij}	5.4^{a}	37.0^{c}
	Thyolo	52.5^{ef}	59.3^{klm}	65.8^{fgh}	13.3^{j}	4.2^{def}	27.4^{ij}
	Zomba	52.9^{e}	60.4^{de}	66.1^{def}	13.3^{j}	4.8^{b}	35.1^{cd}
	Mean	50.8±2.3	58.9±1.3	65.3±1.3	14.4±1.3	4.4±0.7	34.5±7.4
Sweetpotato	A45	49.2^{l}	58.2^{o}	65.7^{fgh}	16.5^{abc}	3.2^{k}	24.9^{l}
	Babache	50.0^{k}	59.1^{lm}	66.8^{bcd}	16.8^{a}	4.1^{f}	32.9^{def}
	Kakoma	51.3^{ij}	59.6^{ij}	66.0^{efgh}	14.6^{fghi}	3.6^{ghi}	36.2^{c}
	Kamchiputu	52.1^{fgh}	59.7^{hi}	65.8^{fgh}	13.7^{ij}	2.9^{l}	25.2^{kl}
	Kenya	52.2^{fg}	60.0^{fg}	66.3^{cdef}	14.1^{ghij}	3.4^{ghi}	27.3^{jk}
	LU96/303	52.0^{fgh}	60.2^{ef}	66.8^{bcd}	14.8^{efgh}	4.4^{cde}	31.5^{efg}
	LU96/304	51.4^{hij}	60.6^{d}	67.0^{bc}	15.6^{cdef}	4.2^{ef}	36.0^{c}
	Lunyangwa	49.5^{kl}	58.5^{n}	65.5^{fgh}	16.0^{abcd}	3.3^{jk}	30.0^{ghi}
	Mafutha	51.8^{ghij}	59.9^{gh}	66.6^{bcde}	14.8^{efgh}	3.6^{ghi}	30.2^{fg}
	Mugamba	52.4^{efg}	60.5^{d}	67.1^{b}	14.7^{fghi}	4.4^{cd}	37.0^{c}
	Mugande	53.9^{cd}	61.4^{b}	67.4^{ab}	13.5^{j}	3.6^{ghi}	29.9^{ghi}
	Salera	53.6^{d}	61.1^{c}	67.4^{ab}	13.8^{ij}	3.7^{gh}	30.7^{fg}
	Semusa	54.1^{bcd}	61.7^{a}	68.0^{a}	13.9^{hij}	4.5^{c}	33.4^{de}
	Tainoni	54.8^{a}	61.6^{ab}	66.8^{bcd}	12.0^{k}	3.5^{ghi}	28.1^{hij}
	Zondeni	50.0^{k}	59.4^{jk}	65.7^{fgh}	15.7^{bcde}	3.4^{ijk}	29.5^{ghij}
	Mean	51.8±1.7	60.1±1.1	66.6±0.8	14.7±1.4	3.7±0.5	30.9±3.8
Cassava	Gomani	54.3^{abc}	59.3^{jkl}	63.4^{i}	9.1^{l}	1.1^{n}	7.9^{n}
	Maunjili	54.6^{ab}	59.7^{hi}	63.9^{i}	9.2^{l}	1.6^{m}	10.6^{m}
	Mbundumali	54.4^{abc}	59.7^{hi}	64.0^{i}	9.2^{l}	1.6^{m}	11.9^{m}
	Mkondezi	54.7^{ab}	59.7^{hi}	63.7^{i}	9.0^{l}	1.4^{m}	10.5^{m}
	Sauti	54.6^{ab}	59.5^{ijk}	63.8^{i}	9.2^{l}	1.1^{n}	8.0^{n}
	Mean	54.5±0.2	59.6±0.2	63.8±0.4	9.2±0.4	1.4±0.2	9.8±1.8

Means followed by the same letter within the same row are not significantly different from each other ($p \leq 0.05$); Mean for botanical source are expressed as mean ±SD.

power, gelatinisation temperatures, syneresis and degree of retrogradation. Cassava starches exhibited higher paste clarity, viscosity, water binding capacity and swelling power but lower gelatinisation temperatures, syneresis and degree of retrogradation (Figure 2). Principal component 2 contrasted cassava and cocoyam starches with sweetpotato starches with respect to gelatinisation enthalpy, swelling power and water binding capacity: Cassava and cocoyam starches displayed higher gelatinisation enthalpy, swelling power and water binding capacity than sweetpotato starches (Figure 2).

The factor loading revealed that cassava starches were contrasted with cocoyam starches in terms of high paste clarity, viscosity, water binding capacity and swelling power, lower gelatinisation temperatures and lower degree of retrogradation and syneresis. The plot also showed that that cocoyam starches (Nkhotakota, Zomba, Mulanje and Machinga) had the lowest negative scores. These starches were discriminated in terms of their higher degree of syneresis and retrogradation, higher gelatinization temperatures and lower water absorption capacity, swelling power, viscosity and paste clarity.

The correlation matrix (Table 9) showed that swelling power, water binding capacity, viscosity and paste clarity were closely related. These variables were positively correlated. On the other hand gelatinisation temperatures (T_o, T_p) and syneresis were also close to each other. Kong et al. (2009) also reported significant positive correlation between gelatinization temperatures, T_o, T_p, and T_c and the enthalpy. There was significant negative correlation between swelling power, water binding capacity, viscosity and paste clarity with gelatinisation

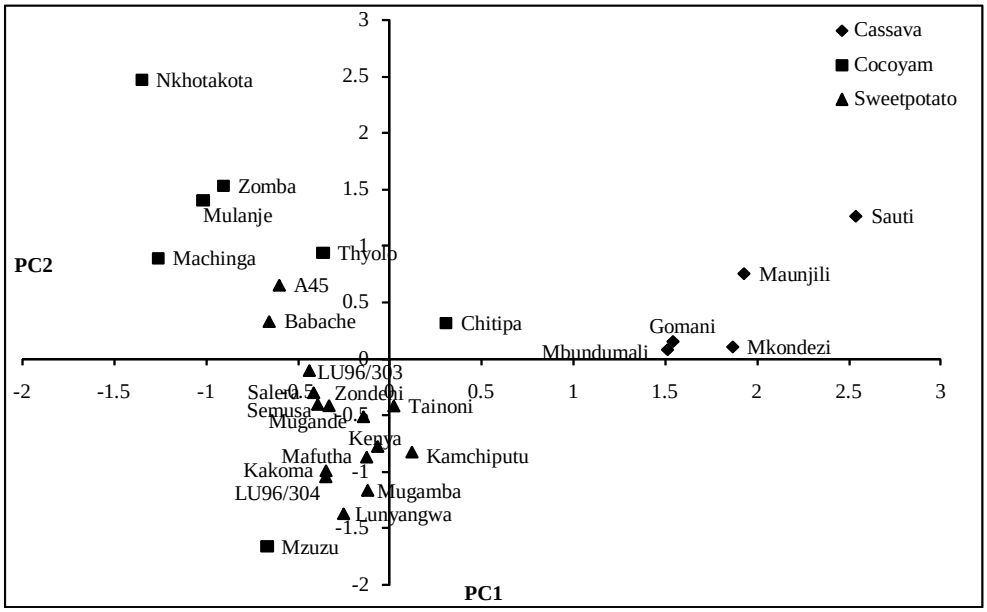

Figure 1. PC1 and PC2 plot for cocoyam, sweetpotato and cassava starches.

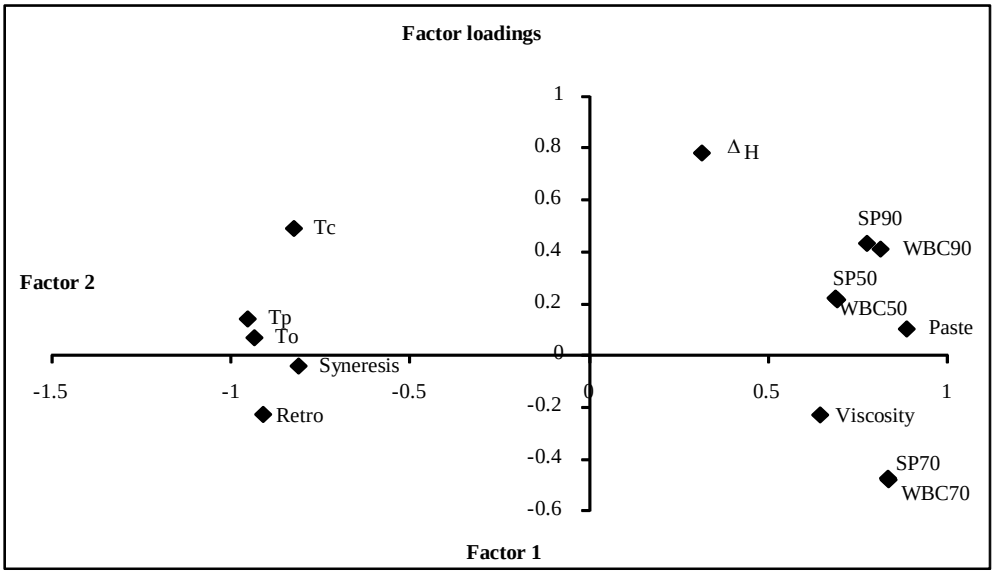

Figure 2. PCA loading plot for functional properties of the cocoyam, sweetpotato and cassava starches.

temperatures (T_o, T_p, T_c), retrogradation and syneresis.

This is in agreement with results of Singh et al. (2006), who reported a significant correlation between swelling power and gelatinization temperatures, and syneresis. However, swelling power was negatively correlated with setback viscosity. Singh et al. (2004) also reported positive correlation between swelling power and light transmittance, peak and conclusion gelatinisation temperatures but a negative correlation with water binding capacity.

Conclusions

The results of this study have revealed differences in functional properties of starches from cassava, sweetpotato and cocoyam grown in Malawi. Cassava starches were contrasted with cocoyam and sweetpotato

Table 8. Principal component analysis of the functional properties of the cocoyam accessions, sweetpotato and cassava starches.

Variable	Eigenvectors		
	PC1	PC2	PC3
Paste	0.30	0.07	0.12
To	-0.31	0.05	-0.07
Tp	-0.32	0.10	-0.06
Tc	-0.28	0.36	0.00
ΔH	0.11	0.57	0.11
Retro	-0.31	-0.17	-0.07
WBC50	0.23	0.16	-0.64
WBC70	0.28	-0.35	0.01
WBC90	0.27	0.30	0.25
SP50	0.23	0.16	-0.63
SP70	0.28	-0.34	0.03
SP90	0.26	0.31	0.27
Viscosity	0.22	-0.16	0.12
Syneresis	-0.27	-0.03	-0.02
Eigen values	8.9	1.9	1.2
Individual %	63.4	13.6	8.3
Cumulative %	63.4	77.0	85.3

Table 9. Correlation coefficients between the functional parameters of the cocoyam, sweetpotato and cassava starches.

	Paste	To	Tp	Tc	ΔH	Retro	WBC50	WBC70	WBC90	SP50	SP70	SP90	Viscosity
To	-0.83**												
Tp	-0.80**	0.97**											
Tc	-0.64**	0.82**	0.88**										
ΔH	0.30	-0.23	-0.17	0.13									
Retro	-0.76**	0.85**	0.86**	0.65**	-0.54**								
WBC50	0.55**	-0.57**	-0.58**	-0.46*	0.28	-0.61**							
WBC70	0.67**	-0.82**	-0.85**	-0.90**	-0.01	-0.66**	0.45						
WBC90	0.81**	-0.76**	-0.75**	-0.49**	0.48*	-0.80**	0.49*	0.46					
SP50	0.56**	-0.58**	-0.59**	-0.47*	0.27	-0.60**	1.0**	0.46	0.49**				
SP70	0.67**	-0.83**	-0.85**	-0.90**	-0.01	-0.65**	0.46	1.0**	0.46	0.44			
SP90	0.80**	-0.74**	-0.72**	-0.45*	0.47*	-0.76**	0.49**	0.42	0.99**	0.46	0.43		
Viscosity	0.62**	-0.43	-0.57**	-0.59**	0.11	-0.53**	0.3	0.60**	0.42	0.32	0.59**	0.36	
Syneresis	-0.71**	0.66**	0.70**	0.61**	-0.33	0.81**	-0.53**	-0.64**	-0.61**	-0.53**	-0.62**	-0.54**	-0.65**

*, ** significant at p = 0.05 and p = 0.01, respectively.

starches as having water binding capacity, swelling power, paste clarity, viscosity, and resistance to retrogradation and lower gelatinisation temperatures. Cocoyam starches were characterised by higher degree of retrogradation and syneresis, and lower paste viscosity; sweetpotato starches displayed intermediate properties. Thus cassava starches could be explored for various applications use in the food and adhesive. Modification of cocoyam and sweetpotato could help improve their functional properties for specific use in the starch based industry.

Conflict of Interest

The authors have not declared any conflict of interest.

ACKNOWLEDGEMENT

This research work was supported by the International Program in Chemical Sciences-International Science Program (IPICS-ISP), Uppsala University, Sweden through the Malawi project-Genetics and Chemistry of Root and Tuber Crops in Malawi (MW01). The author would like to thank the IPICS-ISP for the financial support towards this project.

REFERENCES

Adebowale KO, Lawal OS (2002). Effect of annealing and heat moisture conditioning on the physicochemical characteristics of Bambara groundnut (*Voandzeia subterranean)* starch and flour. Food Chem. 78:305-311.

Amani N'GG, Buléon A, Kamenan A, Colonna P (2004). Variability in starch physicochemical and functional properties of yam (*Dioscorea sp*) cultivated in Ivory Coast. J. Sci. Food. Agric. 84:2085-2096.

Bello-Pérez LA, Contreras-Ramos SM, Jimenez-Aparicio A, Paredes-Lopez O (2000). Acetylation and Characterization of Banana (*Musa paradisiaca*) starch. Acta Cient. Ven. 51:143-149.

Bentacur-Ancona DA, Chel-Guerrero SLA, Camelo-Matos RI, Davila-Ortiz G (2001). Physicochemical and functional characterisation of baby lima bean (*Phaseolus lunatus*) starch. *Starch/Stärke* 53:248-254.

Brook JR, Griffin JK, Kattan W (1986). A modified method for total carbohydrate analysis of glucose syrups, maltodextrins and other starch hydrolysis products. Cereal Chem. 63(5):465-467.

Craig SAS, Maningat CC, Seib PA, Hoseney RC (1989). Starch paste clarity. Cereal Chem. 66:173-182.

De la Torre-Gutiérrez L, Chel-Guerrro LA, Betancur-Ancona D (2008). Functional properties of square banana (*Musa babisiana*) starch. Food Chem. 106:1138-1144.

Ellis RP, Cochrane MP, Dale MFB, Duffus CM, Lynn A, Morrison IM, Prentice RDM, Swanston JS, Tiller SA (1998). Starch production and industrial use. J. Sci. Food Agric. 77:289-311.

Gbadanosi SO, Oladeji BS (2013). Comparative studies of the functional and physico-chemical properties of isolated cassava, cocoyam and breadfruit starches. IFRJ. 20(5):2273-2277.

Gudmundsson M (1994). Retrogradation of starch and the role of its components. Thermochim. Acta 246(2):329-341.

Gujska E, Reinhard WD, Khan R (1994). Physicochemical properties of field pea, pinto and navy bean starches. J. Food Sci. 59:634-636.

Gunaratne A, Hoover R (2002). Effect of heat-moisture treatment on the structure and physicochemical properties of tuber and root starches. Carbohydr. Polym. 49:425-437.

Hoover R, Sosulski F (1986). Effect of cross linking on functional properties of legume starches. Starch/Stärke 38: 149-155.

International Starch Institute (2002). ISI 17-1e. Determination of viscosity of starch by Brookfield Viscometer.

Jacobson MR, Obanni M, Bemiller JN (1997). Retrogradation of starches from different botanical sources. Cereal Chem. 66:173-182.

Jane J, Chen YY, Lee LF, McPherson AE, Wong KS, Radosavljevic M (1999). Effects of Amylopectin Branch Chain Length and Amylose Content on the Gelatinization and Pasting Properties of Starch. Cereal Chem. 76(5):629-637.

Jane J, Kasemsuwan T, Chen JF (1996). Phosphorus in Rice and Other Starches. Cereal Food. World 41(11):827-832.

Karim AA, Norziah MH, Seow CC (2000). Methods for the study of starch retrogradation. Food Chem. 71:9-36.

Kojima M, Shimizu H, Ohashi M, Ohba K (2006). Physico-chemical Properties and Digestibility of Pulse Starch after Four Different Treatments. J. Appl. Glycosci. 53(2):105-110.

Kong X, Bao J, Corke H (2009). Physical properties of amaranthus starch. Food Chem. 113:271-376.

Krueger BR, Knutson CA, Inglett GE, Walker CE (1987). A differential scanning calorimetry study on the effect of annealing on gelatinization behaviour of corn starch. J. Food Sci. 52:715-718.

Mishra S, Rai T (2006). Morphology and functional properties of corn, potato and tapioca starches. Food Hydrocoll. 20:557-566.

Nwokocha LM, Aviara NA, Senan C, Williams PA (2009). A comparative study of some properties of cassava (*Manihot esculenta*, Crantz) and cocoyam (*Colocasia esculenta*, Linn) starches. Carbohydr. Polym. 76(3):362-367.

Otegbayo B, Oguniyan D, Akinwumi O (2013). Physicochemical characteristics and functional characterisation of yam starch for potential industrial applications. *Starch/Stärke* 65:1-16.

Pérez E, Schultz FS, de Delahaye EP (2005). Characterization of some properties of starches isolated from *Xanthosoma sagittifolium* (tannia) and *Colocasia esculenta* (taro). Carbohydr. Polym. 60:139-145.

Peroni FGH, Rocha TS, Franco CML (2006). Some structural and physicochemical characteristics of tuber and root starches. Food Sci. Technol. Int. 12(6):505-513.

Sandhu KS, Singh N (2007). Some properties of corn starches II. Physicochemical, gelatinization, retrogradation, pasting and gel textural propeties. Food Chem. 101:1499-1507.

Sandhu KS, Singh N, Malhi NS (2005). Physicochemical and thermal properties of starches separated from corn produced from crosses of two germ pools. Food Chem. 89:541-548.

Sasaki T (2005). Effect of wheat starch characteristics on the gelatinization, retrogradation and gelation properties. JARQ 39(4):253-260.

Sasaki T, Masuki J (1998). Effect of wheat structure on swelling power. Cereal Chem. 7:525-529.

Schmitz CS, de Simas KN, Joao JJ, de Mello Castanho Amboni RD, Amante ER (2006). Cassava starch functional properties by etherification-hydroxypropylation. Int. J. Food Sci. Technol. 41:681-687.

Shi YC, Seib PA (1992). The structure of four waxy starches related to gelatinization and retrogradation Carbohydr. Res. 227:131-145.

Singh J, McCarthy OJ, Singh H (2006). Physico-chemical and morphological characteristics of New Zealand Taewa (*Maori potato*) starches. Carbohydr. Polym. 64:569-581.

Singh N, Kaur L, Singh J (2004). Relationships between various physicochemical, thermal and rheological properties of starches separated from different potato cultivars. J. Sci. Food Agric. 84(7):714-720.

Spence KE, Jane J (1999). Chemical and physical properties of ginkgo (Ginkgo biloba) starch. Carbohydr. Polym. 40:261-269.

Srichuwong S, Sunarti TC, Mishima T, Isono N, Hisamatsu M (2005). Starches from different botanical sources II: Contribution of starch structure to swelling and pasting properties. Carbohydr. Polym. 62:25-34.

Tian SJ, Rickard JE, Blanshard JM (1991). Physicochemical properties of sweet potato starch. J. Sc. Food Agric. 57:451-491.

Vaclavik VA, Christian EW (2014). Essentials of Food Science. 4th

edition. Food science Text Series. Springer Science and Business Media, New York, USA. (4):39-49.
Wickramasinghe HAM, Takigawa S, Matsuura-Endo C, Yamauchi H, Noda T (2009). Comparative analysis of starch properties of different root and tuber crops of Sri Lanka. Food Chem. 112: 98-103.
Yuan Y, Zhang L, Dai Y, Yu J (2007). Physicochemical properties of starch obtained from *Dioscorea nipponica* Makino comparison with other tuber starches. J. Food Eng. 82:436-442.

academicJournals

Vol. 10(18), pp. 593-599, 30 September, 2015
DOI: 10.5897/SRE2015.6194
Article Number: 86EC06155375
ISSN 1992-2248
Copyright©2015
Author(s) retain the copyright of this article
http://www.academicjournals.org/SRE

Scientific Research and Essays

Full Length Research Paper

Spectra characterization, flavonoid profile, antioxidant activity and antifungal property of *Senecio bifrae* and its copper complex

Azeez L.[1]*, Ogundode S. M.[2], Ganiyu O. T.[3], Oyedeji O. A.[4], Tijani K. O.[5] and Adewuyi S. O.[6]

[1]Environmental, Analytical and Nutritional Chemistry Research Laboratory, Department of Chemical Sciences, Osun State University, Osogbo, Osun State, Nigeria.
[2]Biochemistry and Nutrition Unit, Department of Chemical Sciences, Fountain University, Osogbo, Nigeria.
[3]Microbiology Unit, Department of Biological sciences, Fountain University, Osogbo, Osun State, Nigeria.
[4]Department of Science Laboratory Technology, the Federal Polytechnic, Ilaro, Ogun State, Nigeria.
[5]Industrial and Environmental Chemistry Unit, Department of Chemical Sciences, Fountain University, Osogbo, Osun State, Nigeria.
[6]Department of Pure and Applied Chemistry, Ladoke Akintola University of Technology, Ogbomoso, Oyo State, Nigeria.

Received 20 February, 2015; Accepted 2 September, 2015

This study describes the synthesis, spectra characterization using UV-Visible and Infra-Red spectroscopic methods, flavonoid profile, antioxidant activity and antifungal property of *Senecio biafrae*-Cu complex and *Senecio biafrae*. UV-Visible spectra revealed bathochromic shifts for *Senecio biafrae*-Cu complex in comparison with *Senecio biafrae* which could be due to complexation. Differences between vibration spectra of *Senecio biafrae*-Cu complex and *Senecio biafrae* showed that carbonyl oxygen and hydroxyl groups were involved in complexation because of shifts in their positions. Kaempferol; a flavonol was found to be most abundant identified in both *Senecio biafrae* and its complex. *Senecio biafrae*-Cu complex had better antioxidant and antifungal activities against free radicals and pathogenic *Fusarium oxysporium*, *Aspergillus flavus* and *Fusarium solani* than *Senecio biafrae*. This study has shown that natural vegetables such as *S. biafrae* can also be used for complexation.

Key words: *Senecio biafrae*, flavonoid composition, antifungal property, inhibition, copper complex.

INTRODUCTION

In today's world, it is difficult to avoid exposure to heavy metals such as cadmium, mercury, lead, copper, chromium, nickel e.t.c. They enter into human body through food, water, air and skin. These heavy metals exert their toxic effects by producing free radicals which cause oxidative stress (Azeez et al., 2013). Copper (Cu) is essential for living but it has also been reported to have a major role in the production of the very reactive

*Corresponding author. E-mail: azeez012000@yahoo.com, Tel: +2348061538999.
Author(s) agree that this article remain permanently open access under the terms of the Creative Commons Attribution License 4.0 International License

hydroxyl radical $HO^{\cdot}$ through the Fenton and Haber-Weiss reactions (Puig and Thiele, 2002; Panhwar et al., 2010; Riha et al., 2014). Free radicals such as hydroxyl radical generated by excessive exposure to copper leads to damage that affects lipids, protein/enzymes, carbohydrates, and DNA in cells and tissues (Bukhari et al., 2008). Each organism is imbued with mechanisms to safely excrete the excess Cu ions in the body but when this is hampered, chelation therapy can be used to remove excess Cu ions from vulnerable sites in critical organs (Malešev and Kunti, 2007; Dehghan and Khoshkam, 2012).

Chelation therapy is a promising method in treating pathological diseases arising from oxidative stress caused by excess or dysregulation of transition metals. This is achieved by suppressing the metal induced toxicity (Moridani et al., 2003). Chelating agents such as flavonoids have a natural way of complexing toxic metals and are easily excreted from the body. This plays a major role in limiting metal bioavailability and suppressing metal toxicity and is preferred to synthetic metal chelators because of toxicity (Moridani et al., 2003; Cao et al., 2015; Aaseth et al., 2015)

Flavonoids, a class of phenolic compounds have been shown to possess anti-inflammatory, antiviral, anticarcinogenic, antithrom-botic, antiallergic and hepatoprotective properties (Malesev and Kuntic, 2007). They are extensively distributed in plant-based foods. They are important natural antioxidants and free radical scavengers (Liu, 2003).

Flavonoid-metal complexes have been shown to possess higher antioxidant activity against free radicals and antimicrobial activity against pathogenic microorganisms such as *Staphylococcus aureus*, *Escherichia coli* and *Bacillus cereus* (Pereira et al., 2007; Dehghan and Khoshkam, 2012). Quercetin, morin, rutin kaemferol, naringin, catechin are some of flavonoids that have been used to chelate heavy metals such as Cu and they have proved to be better source of antioxidant (Pereira et al., 2007; Bukhari et al., 2008; Panhwar et al., 2010; Dehghan and Khoshkam, 2012). However, these flavonoids are eaten as part of food in vegetables or fruits but not isolated from them before they are consumed. Moreover, their concentrations in vegetables may differ from those concentrations reported for metal chelation. Hence, the use of vegetables such as *Senecio biafrae* which contain appreciable amounts of these flavonoid compounds (Muhammed et al., 2012). *S. biafrae* is one of the common vegetables consumed in Sierra Leone, Ghana, Benin Republic, Nigeria, Cameroon and Gabon. It is nutritive, rich in protein, ascorbic acid and polyphenols. It is also medicinal and has therapeutical properties. Its leaves contain various secondary metabolites such as dihydroisocoumarins, terpenoids, sesquiterpenes and amino acids (Dairo and Adanlawo 2007; Adefegha and Oboh, 2011).

The purposes of this study were to investigate the chelating property of *S. biafrae*; a source of different flavonoids and characterize *S. biafrae*- copper complex using UV-Visible and Infra Red spectroscopic methods; also, to investigate the antioxidant and antifungal activities of both *S. biafrae* and *S.biafrae*-copper complex.

MATERIALS AND METHODS

Collection of vegetable sample

S. biafrae leaves used for this study were purchased from farm around Olu-Ode market in Osogbo, Osun State, Nigeria. The vegetable was identified and authenticated by Mrs. F.M Tairu at National Horticultural Research Institute (NIHORT), Ibadan with voucher number NIH. 112427. The vegetables were lyophilized, ground, stored in foil paper and kept in a dessicator.

Chemicals

2,2-diphenyl-1-picrylhydrazyl (DPPH), copper sulphate pentahydrate ($CuSO_4.5H_2O$), standard flavonoid compounds, methanol, sodium hydroxide, and aluminum chloride were used. All reagents were analar grade bought from Sigma Aldrich, Germany. Fungal culture, discs and agar were obtained from Microbiology unit, Fountain University, Osogbo. Deionized-distilled water was used all through the experiments.

Extraction

The method of Olajire and Azeez (2011) was used for this extraction. Fifty grams (50 g) of the powdered *S. biafrae* was soaked in 500 ml of 70% aqueous methanol and was shaken on orbital shaker for 4 h. The solution was filtered with Whatman No. 4 filter paper and the filtrate was evaporated at 40°C to dryness using a rotary evaporator.

Synthesis of *S. biafrae*-copper complex

1 g of *S. biafrae* extract was dissolved in 100 ml of methanol and stirred thoroughly until complete dissolution of the extract. 1 g of copper sulphate pentahydrate ($CuSO_4.5H_2O$) was added and the solution turned brownish-green upon stirring for 1hr 30 min. afterwards, the solution was filtered using Whatman No. 4 filter paper and the filtrate was evaporated at 40°C to dryness using rotary evaporator.

Instrumentation

UV–visible spectra of *S. biafrae* extract and *S. biafrae*-Cu complex were obtained using Jenway 6405 UV-Visible spectrophotometer and Infrared spectra were recorded using KBr pellets in the spectral range 4000 to 400 cm^{-1} on FTIR Spectrophotometer (Model 500, Buck Scientific Inc.).

Identification and quantification of flavonoid composition with gas chromatrography-flame ionization detector (GC-FID)

The procedures described by Whitehead et al. (1983) and Provan et al. (1994) were used for the extraction of flavonoids from *S.*

biafrae. Briefly, 50 mg of the sample was extracted with 5 ml of 1 M NaOH for 16 h on a shaker at ambient temperature. After this, the extract was centrifuged (5000 g). The residue was rinsed with deionized water, centrifuged again and the combined supernatants were placed in a disposable glass test tube which was heated at 90°C for 2 h to release conjugated flavonoids. The heated extract was cooled, titrated with 4 M HCl to pH < 2.0, diluted to 10 ml, with deionised water, and centrifuged to remove the precipitate. 15 ml of the supernatant obtained was passed through a conditioned Varian (Varian Assoc., Habor City, CA) Bond Elut PPL (3-ml size with 200 mg packing) solid- phase extraction tube at 5 ml min^{-1} attached to a Visiprep (Supelco, Bellefonte, PA). The tubes were then placed under vacuum (-60 kPa) until the resin was thoroughly dried after which the flavonoids were eluted with 1 mL of ethyl vials. The PPL tubes were conditioned by first passing 2 mL of ethyl acetate followed by 2 ml of water (pH < 2.0).

The composition of flavonoid in *S. biafrae* extract and *S. biafrae*-Cu complex was analyzed using gas chromatography coupled with flame ionization detector (GC-FID). 1 µl of each solution was injected into GC (Hewlett-Packard Model 5890, USA) with FID which has HP-1 column (30 m × 0.25 µm × 0.25 mm id), nitrogen carrier gas, a detector section temperature of 320°C and a split ratio (20:1) mode inlet section (250°C). The column was initially at 60°C held for 5 min and increased at 15°C/ min for 15 min, maintained for 1 min and at 10°C/mi for 4 min held for 2 min. Flavonoids obtained were compared with their standards which were analyzed before the samples. Calibration curves of standard flavonoids analyzed were plotted and good correlation coefficients (r^2) between 0.9992 and 0.9998 were obtained.

Determination of antioxidant activity

The method of Olajire and Azeez (2011) was used for the determination of antioxidant activity. 1, 0.8, 0.6, 0.4 and 0.2% solutions of *S. biafrae* extract and *S.o biafrae*-Cu complex were prepared. 1 ml of each concentration was measured into test tubes and 4 ml of 0.004 M DPPH was added to each tube in a dark room. The blank was prepared by measuring 1 ml of deionized-distilled water in a test tube and 4 ml of DPPH was added. Both blank and samples were allowed to stand for 30 min in dark room before reading at wavelength 517 nm. Percentage Inhibitory for both samples was calculated using this formula:

$$I\,\% = \frac{A_{blank} - A_{sample}}{A_{sample}}$$

Inhibitory concentration at which 50% of the free radicals were scavenged was extrapolated from the graph.

Determination of antifungal activity

The antifungal activity was determined using the poison food technique. Five-day old fungal cultures were punched aseptically with sterile cork borers of 4 mm diameter. The fungal discs were then put on the gelled agar plate. The agar plates were prepared by impregnating them with 100 ppm of ethanolic and aqueous solutions of *S. biafrae* extract and *S. biafrae*-Cu complex at a temperature of 45 to 50°C. The plates were then incubated at temperature of 25°C for fungi growth. The test fungus was then allowed to grow on poisoned plates with ethanolic and aqueous solutions of the extracts. Control tests were carried out simultaneously by putting fungal discs on a gelled agar plates containing 100 ppm of acetic acid as the positive control and 100 ppm of ethanol as the negative control. The effects of *Senecio biafrae* extract and *Senecio biafrae*-Cu on fungal growth were determined by measuring the diameter of the zone of inhibition obtained on poisoned plate and control plates. Percentage inhibition of mycelial growth using the method of Moslem and El-Kholie (2009) was calculated with the formula:

$$\%\ \text{Mycelial inhibition} = \frac{\text{Mycelial growth (control)} - \text{Mycelial growth (treatment)}}{\text{Mycelial growth (control)}}\ X\ 100$$

RESULTS

Flavonoid profile of *S. biafrae* and its Cu complex

Table 1 presents the flavonoid composition in *S. biafrae* extract and *S. biafrae*-Cu complex. In *S. biafrae* extract, the relative abundance of flavonoid compounds followed the trend; Kaempferol > quercetin > isorhamnetin > luteolin > apigenin while other were less than one. In *S. biafrae*-Cu complex, the trend was Kaempferol > isorhamnetin > quercetin > luteolin > apigenin while others were not detected. There were reductions of 56.71% in kaempferol, 83.94% in quercetin, 29.56% in isorhamnetin, 5.90% in luteolin and 45.07% in apigenin concentrations of *S. biafrae*-Cu complex compared with their concentrations in *S. biafrae* extract. This suggests that there was complexation between Cu (II) and the vegetable.

UV-visible spectra characterization of *S. biafrae* and its Cu complex

Figure 1 shows the characteristic peaks of flavonoids in *S. biafrae* extract and *S. biafrae*-Cu complex. In *S. biafrae* extract, absorption maxima (λ_{max}) were observed at 258 nm (Band II) and 375 nm (Band I). Bathochromic shifts in λ_{max} to 277 nm (band II) and 463 nm (band I) were observed in *S. biafrae*-Cu complex.

Vibrational spectra characterization of *S. biafrae* and its Cu complex

The coordination sites and binding properties in *S. biafrae* are presented in Table 2. The stretching vibration of C=O in *S. biafrae* occurred at 1658.05 cm^{-1} which was shifted to 1649.38 cm^{-1} in *S. biafrae*-Cu complex. The shift in O-H was from 3367 cm^{-1} in *S. biafrae* to 3426 cm^{-1} in *S. biafrae*-Cu complex. The bands at 1416.47, 1645 cm^{-1} and 1252.57 cm^{-1} are related to υ(C-OH), υ(C=C) and υ(C-O-C). The presence of υ (Cu-O) was observed at 408.04 cm^{-1} in *S. biafrae*-Cu complex but not in *S. biafrae*.

Antioxidant activity *S. biafrae* and its Cu complex

Figure 2 shows the antioxidant activity of *S. biafrae* extract and *S. biafrae*-Cu complex. *S. biafrae*-Cu

Table 1. Flavonoid composition of *Senecio biafrae* and *Senecio biafrae*-Cu complex.

Flavonoid (mg/100 g)	*Senecio biafrae*	*Senecio biafrae*-Cu complex
Catechin	5.25e-6	ND
Rutin	2.04e-4	ND
Apigenin	3.75	2.06
Luteolin	4.41	4.15
Quercetin	63.31	10.17
Kaempferol	115.22	49.88
Myricetin	6.33e-4	ND
Naringenin	1.53e-3	ND
Epicatechin	2.79e-3	ND
Epicatechin-3-gallate	4.89e-5	ND
Gallocatechin	8.49-4	ND
Isoquercetin	0.21	ND
Kaempferol-3-arabinoside	4.27e-4	ND
Isorhamnetin	17.09	12.05
Orientin	3.82e-4	ND
Isoorientin	0.16	ND
Naringin	5.09e-4	ND
Daidzein	3.91e-4	ND
Morin	1.53e-3	ND
Quercitrin	7.25e-4	ND

ND, Not detected.

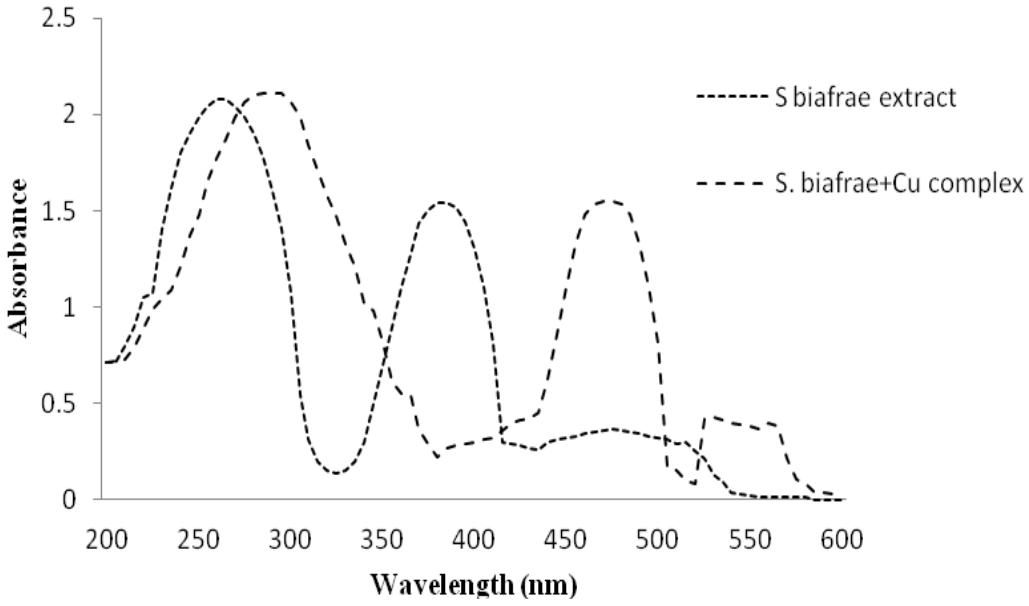

Figure 1. UV-Visible spectra of *Senecio biafrae* and *Senecio biafrae*-Cu extracts.

complex had 89.92% antioxidant activity while *S. biafrae* extract had 64.15%. Antioxidant activity of *S. biafrae*-Cu complex in this study is higher than what Dehghan and Khoshkam (2012) and Pereira et al. (2007) reported for Sn – quercetin and Cu - naringin complexes but lower than what Bukhari et al. (2008) reported Co – quercetin complex. Inhibitory concentration at which 50% of the radicals are scavenged (IC_{50}) for *S. biafrae*-Cu complex is

Table 2. Vibrational spectra bands (cm^{-1}) of *Senecio biafrae* and *Senecio biafrae*-Cu complex.

Bands	*S. biafrae*	*S. biafrae*-Cu
υ (O-H)	3367.00 s	3426.00 s
υ (C=O)	1658.05 s	1649.38 s
υ (C-H)	2947.66 s	
υ (C-OH)	1416.47 m	1402 m
υ (C-O)	1028.48 s	
υ (C=C)	1645.00 s	1631.00 s
υ (C-O-C)	1252.57 s	1212.1 m
υ (Cu-O)		408.04 s

s, Strong; m, medium.

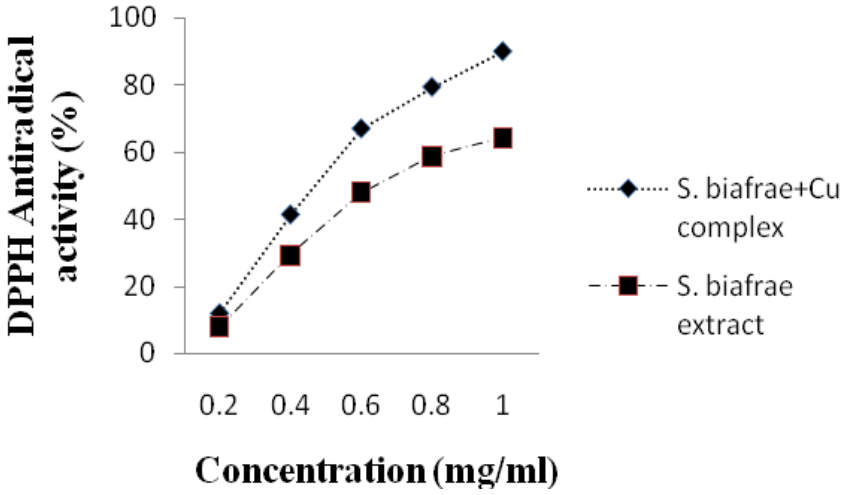

Figure 2. Antiradical efficiency of *S. biafrae* and *S. biafrae*-Cu extracts.

Table 3. Antifungal activity (% mycelia inhibition) of *S. biafrae* and *S. biafrae*-Cu complex.

S/N	Organism	Aq. extract of *S. biafrae*	Aq. extract of *S. biafrae*-Cu	Eth. extract of *S. biafrae*	Eth. extract of .*S biafrae*-Cu
1	*Fusarium oxysporium*	14.3	28.6	62.9	57.1
2	*Aspergillus flavus*	50.0	45.0	55	62.3
3	*Fusarium solani*	17.7	20.6	32.4	35.3

Aq., Aqueous; Eth., ethanolic.

0.45 mg/ml and for *S. biafrae* extract is 0.68 mg/ml.

Antifungal activity of *S. biafrae* and its Cu complex

Table 3 presents the results of antifungal activity of both aqueous and ethanolic *S. biafrae* extract and *S. biafrae*-Cu complex against *Fusarium oxsporium*, *Aspergillus flavus* and *Fusarium solani.* These results are represented as percentage mycelia inhibition. Aqueous *S. biafrae*-Cu complex had better antifungal activity against *F. oxysporium* and *F. solani* than aqueous *S. biafrae* extract while reverse was obtained for *A. flavus*. Ethanolic *S. biafrae*-Cu complex had higher antifungal activity against *A. flavus* and *F. solani* than ethanolic *S. biafrae* extract while otherwise was obtained for *F. oxysporium*. Very high antifungal activity was observed against *F. oxxysporium* and *A. flavus* with ethanolic

extract while average activity was observed against *A. flavus* with aqueous extract. Percentage mycelial inhibition was highest against *F. oxysporium* followed by *A. flavus* and *F. solani*.

DISCUSSION

Vegetables are one of the dietary sources of flavonoids (Erlund, 2004; Olajire and Azeez, 2011). Flavonoids have anticancer, antifungal anti-inflammatory and contribute significantly to antioxidant activities of vegetables (Tapas et al., 2008; Ghasemnezhad et al., 2011). Flavonol; a class in flavonoids dominated the abundance of flavonoid contents in both *S. biafrae* and *S. biafrae*-Cu complex with kaempferol and quercetin. Therefore, it could be inferred that the activity of flavonoids in both the extract and complex was dictated by flavonols. The contents of quercetin and kaempferol show that both *S. biafrae* and its complex have anti-inflammatory, antibacterial, antioxidant and are effective metal chelators (Malesev and Kuntic, 2007; Pereira et al., 2007; Bukhari et al., 2008; Panhwar et al., 2010; Dehghan and Khoshkam, 2012).

UV-Visible spectroscopic method was used to characterize the *S. biafrae* and its complex because each coloured sample has a characteristic absorption. In metal – flavonoid complexes, bathochromic shifts are usually observed in UV-Visible spectra because the complexes are often coloured (Malesev and Kuntic, 2007). The bathochromic shifts observed in the λ_{max} of the brownish - green *S. biafrae*-Cu complex confirm its formation (Bukhari et al., 2008; Dehghan and Khoshkam, 2012). These bathochromic shifts were caused by increased conjugative effects of *Senecio biafrae*-Cu complex (Malesev and Kuntic, 2007). Band I absorption in *S. biafrae* extract is characteristic of flavonol absorption (352 to 385 nm) suggesting that flavonols dominated the flavonoid compounds in the extract (Malesev and Kuntic, 2007).

To further confirm the formation of complex, functional groups used for binding were analyzed using Infra-Red spectroscopic method. The shifts observed in the positions of C=O, OH, υ(C-OH), υ(C=C) and υ(C-O-C) were due to complexation. These shifts suggest there was complexation in *S. biafrae* involving the carbonyl oxygen and hydroxyl group of the flavonoids in the vegetable (Bukhari et al., 2008; Panhwar et al., 2010).

The presence of υ (Cu-O) in *Senecio biafrae*-Cu complex indicates the formation of metal complex whereas it was absent in *S. biafrae* (Panhwar et al., 2010; Dehghan and Khoshkam, 2012).

Antioxidant activity of *S. biafrae* and its complex was determined in terms of their electron donating abilities using DPPH method. This is a suitable parameter to establish free radical scavenging and health status of these samples (Stoilova et al., 2007; Bukhari et al., 2008; Edziri et al., 2011). Higher antioxidant activity and lower IC_{50} of *Senecio biafrae*-Cu complex compared to *S. biafrae* values shows that it possesses higher potency against free radicals than *S. biafrae* because the lower the IC_{50} the more potent the extract is (Olajire and Azeez, 2011). Higher antioxidant activity of the *Senecio biafrae*-Cu complex suggests that Cu (II) has significantly modified the chemical composition of the flavonoids in the vegetables (Bukhari et al., 2008). This could also be due to the decrease in oxidation potential of flavonoid present in the vegetable by Cu (II) complexation thus, making it readily oxidized, more reactive and effective than free *S. biafrae* (Bukhari et al., 2008; Panhwar et al., 2010). This complex possessed better antioxidant activity that Sn – quercetin and Cu – naringin complexes (Dehghan and Khoshkam 2012; Pereira et al., 2007).

Metal complexes have been reported to possess higher antifungal activity than free ligand such as flavonoids and are used to treat infectious diseases (Al-Amiery et al., 2012). Higher antifungal activity of *Senecio biafrae*-Cu complex against pathogenic *F. oxsporium*, *A. flavus* and *F. solani* which have been implicated in the production of toxins could be connected with antifungal agent such as Kaempferol and quercetin present in it (Cho et al., 2008; Gupta et al., 2009; Dahham et al., 2010). The results of different solvent activities affecting the antifungal potency of extract as obtained in the result of this study is in agreement with results of Dahham et al. (2010) who reported that methanolic extract of *Punica granatum* L. was more potent than aqueous extract of the same plant. This shows that ethanolic extract is better utilized as fungicide than aqueous extract. Since fungi cause diseases and the synthetic fungicides use for their control cause environmental and health hazards (Kanwal et al., 2010) ethanolic extract of *S. biafrae*-Cu complex could be employed to kill off fungi.

Conclusion

This study has reported differences in UV-Visible and Infra-Red spectra of *S. biafrae* and its complex. Shifts were observed in the λ_{max} and vibrational frequencies of *S. biafrae* compared with *S. biafrae*-Cu complex. *S. biafrae*-Cu complex had better potency against free radicals and pathogenic *F. oxsporium*, *A. flavus* and *F. solani* than *S. biafrae*.

Conflict of Interest

The authors have not declared any conflict of interest.

REFERENCES

Adefegha SA, Oboh G (2011). Cooking enhances the antioxidant properties of some tropical green leafy vegetables. Afr. J. Biotech. 10(4):632-639.

Aaseth J, Skaug MA, Cao Y, Andersen O (2015). Chelation in metal intoxication. J. Trace Elem. Med. Biol. 31:260-266.
Al-Amiery AA, Kadhum AAH, Mohamad A (2012). Antifungal and Antioxidant Activities of Pyrrolidone Thiosemicarbazone Complexes. Bioinorg. Chem. Appl. ID 795812, pp. 1-6. doi:10.1155/2012/795812
Azeez L, Adeoye MD, Lawal AT, Idris ZA, Majolagbe TA, Agbaogun BKO, Olaogun MA (2013). Assessment of volatile organic compounds and heavy metals in Nigerian-made cosmetics. Anal. Chem.: An Indian J. 12(12):443-448.
Bukhari SB, Memona S, Tahir MM, Bhanger MI (2008). Synthesis, characterization and investigation of antioxidant activity of cobalt–quercetin complex. J. Mol. Struct. 892:39-46.
Cao Y, Skaug MA, Andersen O, Aaseth J (2015). Chelation therapy in intoxications with mercury, lead and copper. J. Trace Elem. Med. Biol. 31:188-192. DOI: http://dx.doi.org/10.1016/j.jtemb.2014.04.010
Cho S, Lee C, Jang M, Son Y, Lee S, Choi I, Kim S, Kim D (2008). Aflatoxins contamination in spices and processed spice products commercialized in Korea. Food Chem. 107:1283-1288.
Dahham SS, Ali MN, Tabassum H, Khan M (2010). Studies on Antibacterial and Antifungal Activity of Pomegranate (*Punica granatum L.*). American-Eurasian J. Agric. Environ. Sci. 9(3):273-281.
Dairo FAS, Adanlawo IG (2007). Nutritional quality of *Crassocephalum crepidioides* and *Senecio biafrae*. Pak. J. Nutr. 6:35-39.
Dehghan G, Khoshkam Z (2012). Tin (II)–quercetin complex: Synthesis, spectral characterisation and antioxidant activity. Food Chem. 131:422-426.
Edziri HL, Smachd MA, Ammarc S, Mahjoub MA, Mighric Z, Aounia M, Mastourib M (2011). Antioxidant, antibacterial, and antiviral effects of *Lactuca sativa* extracts. Ind. Crops Prod. 34:1182-1185.
Erlund I (2004). Review of the flavonoids quercetin, hesperetin, and naringenin. Dietary sources, bioactivities, bioavailability, and epidemiology. Nutr. Res. 24:851-874.
Ghasemnezhad M, Sherafati M, Payvast GA (2011). Variation in phenolic compounds, ascorbic acid and antioxidant activity of five coloured bell pepper *Capsicum annum* fruits at two different harvest times. J. Funct. foods 3:44-49
Gupta VK, Misra AK, Gaur R, Pandey R, Chauhan UK (2009). Studies of genetic polymorphism in the isolates of *Fusarium solani*. Aust. J. Crop Sci. 3(2):101-106.
Kanwal Q, Hussain I, Siddiqui HL, Javaid A (2010). Antifungal activity of flavonoids isolated from mango (*Mangifera indica* L.) leaves. Nat. Prod. Res. 24(20):1907-1914.
Liu RH (2003). Health benefits of fruits and vegetables are from additive and synergistic combination of phytochemicals. Am. J. Clin. Nutr. 78:517-520.
Malešev D, Kunti V (2007). Investigation of metal–flavonoid chelates and the determination of flavonoids via metal–flavonoid complexing reactions. J. Serb. Chem. Soc. 72(10):921-939.
Moridani MY, Pourahmad J, Bui H, Siraki A, O'Brien PJ (2003). Dietary flavonoid iron complexes as cytoprotective superoxide radical scavengers. Free Rad. Biol. Med. 34:243-253.
Moslem MA, El-Kholie EM (2009). Effect of Neem (*Azardirachta indica A Juss*) seed and leaves extract on some plant pathogenic fungi. Pak. J. Bio. Sci. 12(14):1045-1048.
Muhammed AO, Adekomi DA, Tijani AA (2012). Effects of aqueous crude leaf extract of *Senecio biafrae* on the histology of the frontal cortex, kidney, liver and testis of male sprague dawley rats. Sci. J. Bio. Sci. 1(1):13-18.
Olajire AA, Azeez L (2011). Total antioxidant activity, phenolic, flavonoid and ascorbic acid contents of Nigerian Vegetables. Afr. J. Food Sci. Technol. 2(2):022-029.
Panhwar QK, Memon S, Bhanger MI (2010). Synthesis, characterization, spectroscopic and antioxidation studies of Cu(II)–morin complex. J. Mol. Struct. 967:47-53.
Pereira RMS, Andrades NED, Paulino N, Sawaya ACHF, Eberlin MN, Marcucci MC, Favero GM, Novak EM, Bydlowski SP (2007). Synthesis and characterization of a metal complex containing Naringin and Cu, and its antioxidant, antimicrobial, anti-inflammatory and tumor cell cytotoxicity. Molecules 12:1352-1366.
Provan GJ, Scobbie L, Chesson A (1994). Determination of phenolic acids in plant cell walls by microwave digestion. J. Sci. Food Agric. 64:63-65.
Puig S, Thiele DJ (2002). Molecular mechanism of copper uptake and distribution. Curr. Opin. Chem. Biol. 6:171-180.
Rıha M, Karlickov J, Filipsky T, Macakov K, Rocha L, Bovicelli P, Silvestri P, Saso L, Jahodar L, Hrdina R, Mladenka P (2014). In vitro evaluation of copper-chelating properties of flavonoids. RSC Adv. 4:32628-32638.
Stoilova I, Krastanov A, Stoyanova A, Denev P, Gargova S (2007). Antioxidant activity of a ginger extract *Zingiber officinale*. Food Chem. 102:764-770
Tapas AR, Sakarkar DM, and Kakde RB (2008). Flavonoids as Nutraceuticals: A review: Trop. J. Pharm. Res. 7(3):1089-1099.
Whitehead D, Dibb CH, Hartley RD (1983). Bound phenolic compounds in water extracts of soil, plant roots and leaf litter. Soil Biol. Biochem. 15:133-136.

academicJournals

Vol. 10(18), pp. 600-609, 30 September, 2015
DOI: 10.5897/SRE2015.6266
Article Number: 04FE68B55379
ISSN 1992-2248
Copyright©2015
Author(s) retain the copyright of this article
http://www.academicjournals.org/SRE

Scientific Research and Essays

Full Length Research Paper

Influence of Indian Ocean zonal circulation on variability and predictability of Ethiopia highlands vegetation

Mark R. Jury

University Puerto Rico Mayaguez, PR 00681, USA.
University Zululand, KwaDlangezwa 3886, South Africa.

Received 26 May, 2015; Accepted 10 September, 2015

The vegetation fraction over the Ethiopian highlands exhibits large seasonal and multi-annual variability in the period 1982 to 2014. Northern areas are more sensitive to rainfall due to the brevity of the wet season. Differences in the regional climate during periods of high and low vegetation are analyzed using composite fields of rainfall, wind, humidity, sea temperatures, salinity and currents; and correlations at six-month lead-time. The key climatic driver of vegetation is the zonal overturning atmospheric circulation linking subsidence over the east Indian Ocean and ascent within an expanded African monsoon. Certain aspects of this Walker Cell reflect Pacific ENSO interaction with the Indian Ocean Dipole. During cold phase ENSO an upwelling Rossby wave and cool sea temperatures in the west Indian Ocean promote vegetation growth in the Ethiopian highlands.

Key words: Vegetation, climate forcing, prediction, Ethiopia.

INTRODUCTION

Semi arid parts of Africa bordering the Congo monsoon, such as the Sahel and Zambezi, are characterised by high rainfall variability and low yield agriculture that contribute to food insecurity (Cassel-Gintz et al., 1997). To better understand how summer rainfall affects crop production at state-level, past work has compared time series of farm yields, rain-gauge and satellite data (Tucker, 1979; Eklundh, 1998; Richard and Poccard, 1998; Al-Bakri and Suleiman, 2004; Budde et al., 2004). Remotely sensed color reflectance is used to quantify vegetation fraction since 1982 (Bannari et al., 1995), with bias correction for sensor degradation, orbital drift and atmospheric contamination (Chappell et al., 2001; Kawabata et al., 2001; Mennis, 2001; Tucker et al., 2005), and intercomparisons with crop yield (Lewis et al., 1998; Maselli et al., 2000). Rainfall in semi-arid zones drives vegetation growth at seasonal and multi-annual time scales (Budde et al., 2004; Eklundh and Sjöström, 2005; Li et al., 2004; Vanacker et al., 2005) with a response lag of one to two months (Davenport et al., 1993; Eklundh, 1998; Richard and Poccard, 1998). Correlations between vegetation fraction and rainfall are higher for running sums and in zones with a single wet season of 600 to 1000 mm (Davenport et al., 1993; Reed

*Corresponding author. E-mail: mark.jury@upr.edu
Author(s) agree that this article remain permanently open access under the terms of the Creative Commons Attribution License 4.0 International License

et al., 1994; White, 1997; Herrmann et al., 2005;Vanacker et al., 2005; Zhang et al., 2005); whereas vegetation sensitivity to climate in desert and monsoon regions is limited.

Previous research has shown that the El Niño/Southern Oscillation (ENSO) modulates vegetation across Africa (Ropelewski and Halpert, 1987; Myneni et al., 1996; Kogan, 1998; Verdin et al., 1999; Plisnier et al., 2000; Mennis, 2001; Anyamba et al., 2002). Changes in tropical Pacific Ocean sea surface temperatures (SST) influence the overlying atmospheric convection and zonal circulation, with effects spreading globally across the Atlantic and Indian Oceans. Interaction between winds in the western Pacific and SST in the Indian Ocean can modulate ENSO onset or decay (Annamalai et al., 2005; Kug et al., 2005, 2006). In addition to the basin-wide signal forced by ENSO through the Walker circulation, air–sea coupling across the Indian Ocean generates a dipole mode (Saji et al., 1999), with opposing sea temperature anomalies linked by changes in the ocean circulation and Rossby wave activity (Annamalai et al., 2005).

When there is cold water upwelling in the eastern Pacific, the zonal atmospheric circulation generates rising motion over the western Pacific and Africa, every 3 to 7 years (Carleton, 1998; Young and Harris, 2005). Africa's vegetation responds to summer rainfall anomalies forced by ENSO (Ropelewski and Halpert, 1987); being more favourable to crop production during cold phase (Cane et al., 1994; Myneni et al., 1996; Mennis, 2001; Anyamba et al., 2002). Correlations between area-averaged vegetation and global SST have revealed ENSO signals, particularly for southern Africa where the summer rainfall coincides with mature ENSO phase (Anyamba and Eastman, 1996; Myneni et al., 1996; Kogan, 1998; Richard and Poccard, 1998; Anyamba et al., 2001). However links with North Africa are somewhat obscure and unpredictable, as the wet season (June-September) precedes ENSO maturity.

The main goals here are to understand the controls on late summer vegetation in Ethiopia's crop growing region and its links with global climate.

DATAS AND METHODS

The analysis scheme used to uncover the climatic drivers of Ethiopian vegetation is described. Our basis is the bias-corrected July to October satellite vegetation fraction (NDVI) from 1982 to 2014 (Huete et al., 2002; Tucker et al., 2005; Philippon et al., 2014) averaged over the Ethiopian highlands (box in Figure 1a). Atmosphere and ocean reanalysis fields are studied for patterns both simultaneously and in precursor season.

The target area is defined by crop production areas known to the Ethiopian Institute for Agricultural Research and the US Department of Agriculture, encompassing a zone 7-14N, 36.5 to 40.5E (Figure 1a) where vegetation fraction reaches 0.4 following the annual cycle of rainfall (Figure 1b and c). The Jun-Sep rainfall correlation with July to October vegetation is highest in the northern sector (Tigray), where the uni-modal wet season is short (Figure 1d). Temporal lag correlations are greatest from 0 to 3 months (Figure 1e); while correlations with temperature are negative (not shown). Hence the northern highlands are more vulnerable to fluctuations of climate, and the focus of this study. The southern highlands have a bi-modal rainy season and vegetation fraction tends to be steadier and less sensitive to rainfall.

Vegetation fraction may be considered a proxy for Ethiopian crop yield, based on earlier validations (Jury, 2013). Drivers of the in-season (Jul-Oct) climate are studied by composite analysis of high vegetation minus low vegetation years: 1986, 1988, 1994, 1999, 2001, 2002 minus 1983, 1991, 1993, 1998, 2010, 2013. The difference field of GPCP rainfall (Adler et al., 2003) reflects a dipole between Africa and the Indian Ocean, so the area of composite analysis is 20S to 30N, 0 to 120E for maps, and 10S to 20N and 10 to 90E for vertical sections. Parameters include NCEP2 atmosphere reanalysis (Kanamitsu et al., 2002) humidity and zonal circulation, and NOAA ocean reanalysis (Behringer et al., 2007) temperature, salinity and zonal circulation. The composite methods are similar to Hastenrath (2000). A hovmoller analysis of 6-month running mean NOAA satellite outgoing longwave radiation (OLR) anomalies is made in the 10S to 20N latitude band 1982 to 2014, to investigate zonal propagation and dipole features. A useful attribute of OLR is its ability to reveal both convective (-) and subsident (+) weather.

Forecasts in April would be most useful for agricultural planning, so statistical predictors are drawn from the preceding December to March (winter) season. The July to October vegetation fraction is employed to 'find' predictors in global fields by correlation of December to March sea surface temperature (SST) from the Hadley Centre (Kennedy et al., 2011), and sea level pressure (SLP) and 850 hPa winds from the European Community Medium-range Weather Forecast (ECMWF) reanalysis (Dee et al., 2011). All time series are standardized and linearly detrended. Field correlations < 0.28 are deemed insignificant at 90% confidence and shaded neutral in this analysis Table 1.

Predictors were assembled from the 4 to 7 month lead-time correlation maps. The candidate predictor pool was eight over a training period of 32 years: 1982 to 2014. A statistical algorithm was formulated in MSexcel via backward stepwise linear regression onto the target time series. Initially all predictors were included and their partial correlation was evaluated. Those with lower significance (or co-linearity) were screened out and the algorithm was re-calculated with the remaining variables. Its performance was evaluated by r^2 fit, adjusted for the number of predictors. The time series have minimal persistence; statistical significance is achieved with r^2 fit > 0.42 with 31 degrees of freedom. Predicted vs observed scatterplots were analyzed for slope, tercile hits and outliers.

RESULTS

Drivers of in-season vegetation

The GPCP rainfall composite difference map for high minus low vegetation (Figure 2a) reflects a dipole between increased convective rainfall across Africa and dry weather over the east Indian Ocean, consistent with earlier work (Saji et al., 1999; Jury and Huang, 2004, Luo et al., 2010). The African monsoon that is most intense over the Congo basin, tends to expand. Hovmoller analysis of satellite OLR anomalies in latitudes of Ethiopia (Figure 2b) exhibit weak or eastward propagation

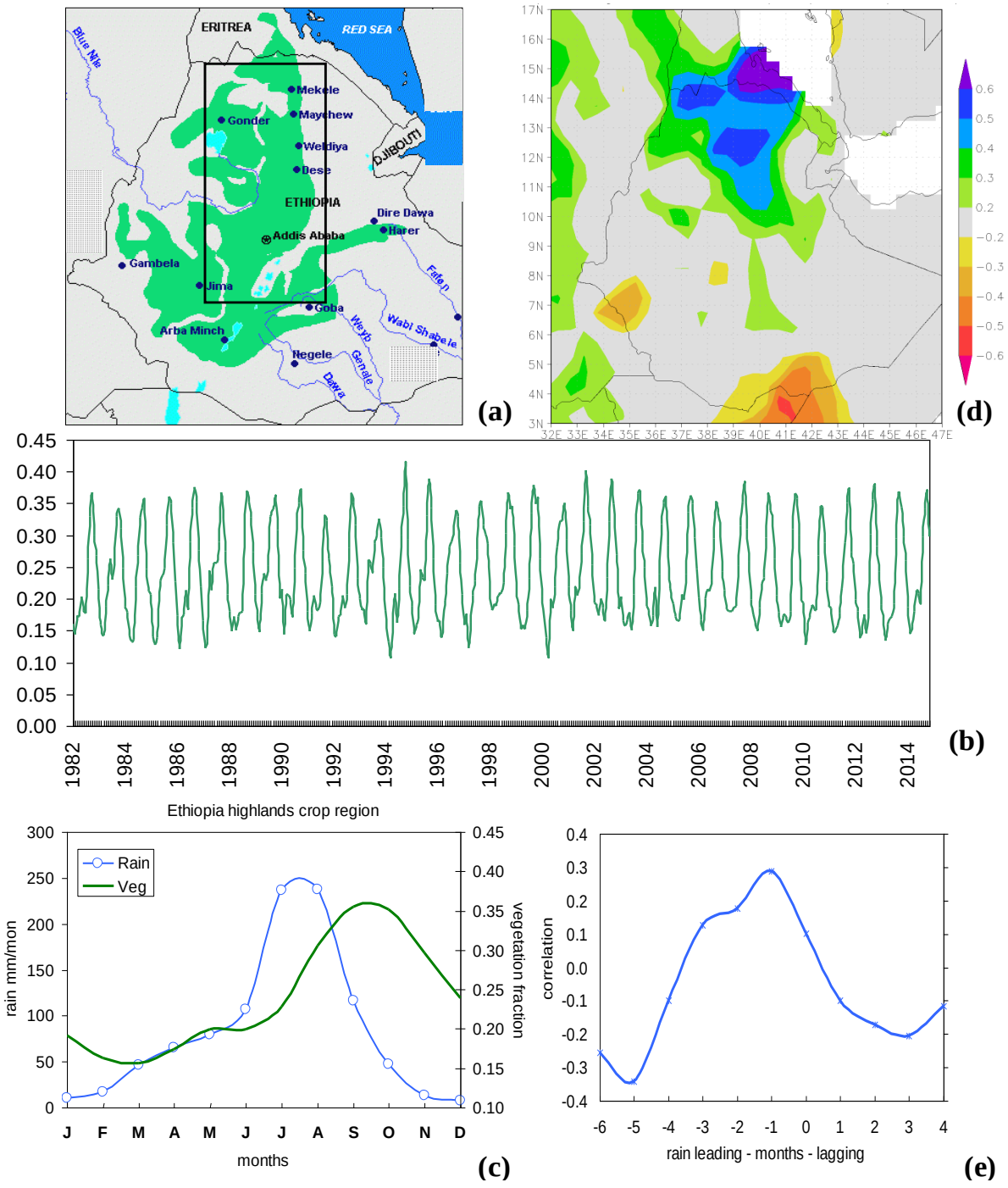

Figure 1. (a) Crop production area of the Ethiopian highlands and target area (box), (b) time series of vegetation index, (c) mean annual cycle of rainfall and vegetation fraction in the target area, (d) correlation map of Jun-Sep rainfall with Jul-Oct vegetation, (e) temporal correlation of local rainfall at various leads and lags and July-Oct vegetation. July t9 October vegetation is plotted in Figure 6a.

of sustained convective features; dipole conditions are seen over the Indian Ocean less than half the time.

The height section of composite high minus low humidity and zonal circulation reflects a dry zone southeast of India where subsidence is found (Figure 3a and b), and a wet zone over Africa where uplift is evident.

Table 1. Datasets used in the statistical analysis. References are listed in text, web sources are given in acknowledgement.

	Name	Resolution (km)
ECMWF	European Centre for Medium-Range Weather Forecasts (interim) Reanalysis	80
GPCP2	Global Precipitation Climatology Project v2 satellite-gauge rainfall	200
NCEP2	National Centers for Environmental Prediction v2 Reanalysis	180
NDVI	Normalized Difference Vegetation Index (NASA)(bias-corrected)	30
NOAA	Global Ocean Data Assimilation System (Reanalysis)	70
OLR	Outgoing Long-wave Radiation from NOAA satellite (bias-corrected)	200 km
SST	Hadley Centre satellite-ship Reanalysis of sea surface temperature	100 km

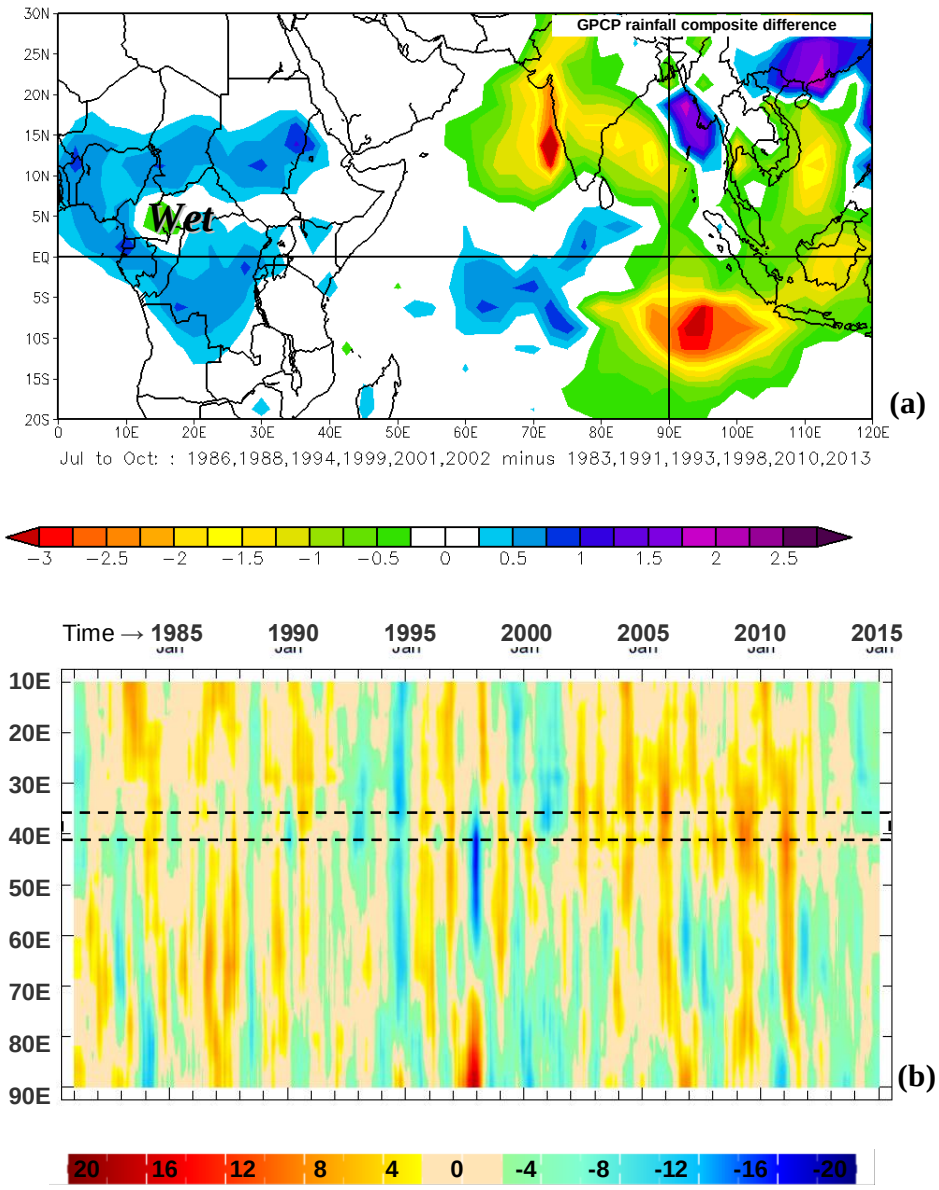

Figure 2. (a) Composite high minus low (vegetation) difference of Jul-Oct GPCP satellite rainfall (mm/day). (b) Hovmoller analysis of satellite OLR anomalies (W/m^2) averaged 10S-20N, with dashed area of Ethiopia.

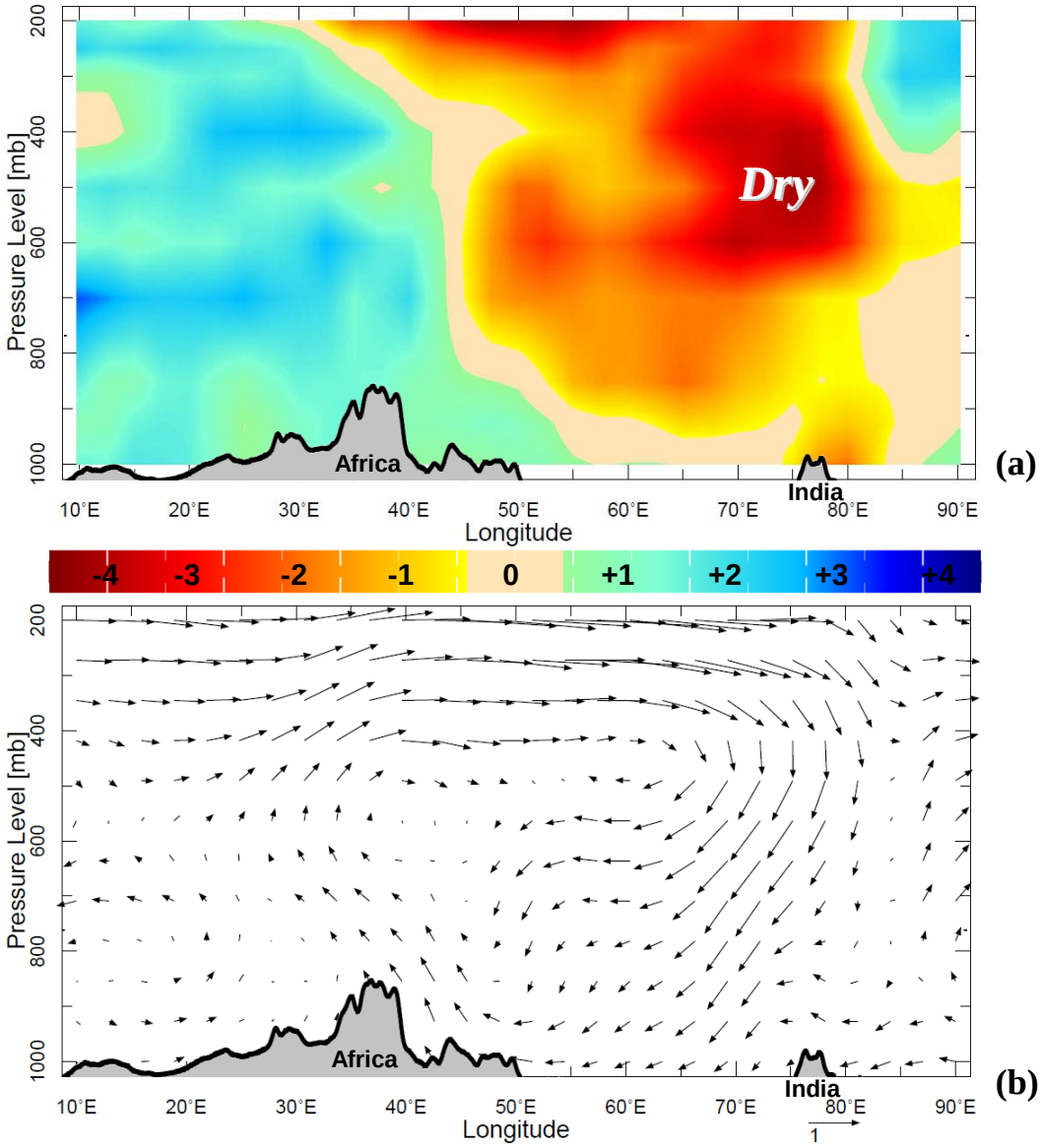

Figure 3. Composite high minus low (vegetation) difference of July to October atmospheric (a) relative humidity (%) and (b) zonal circulation (m/s), in height section averaged 10S-20N with topography.

Surface easterly / upper westerly wind differences complete the zonal overturning atmospheric circulation. The upper ocean composite difference patterns (Figure 4a to c) show a cool anomaly in 40-100 m depths 40 to 65E, and a warm anomaly 60 to 120 m 75-90E, a pattern consistent with Indian Ocean Dipole during Pacific La Niña. The zonal ocean circulation differences reflect westward flow at depth that upwells at 50E. Above the warm zone in the east Indian Ocean near-surface current differences are also westward, but near Africa they are eastward and thus convergent in the central basin. Fresh waters are noted off Africa that correspond with surplus rainfall and run-off, but extend to depths of 300 m.

Elsewhere in the east Indian Ocean, salinity differences are positive above 60m, consistent with evaporation exceeding precipitation there.

Lag correlation and prediction

The July to October vegetation values (1982-2014) are correlated with global fields in December to March season to generate predictor maps (Figure 5a to c). SST fields in respect of vegetation exhibit a cooler west Indian

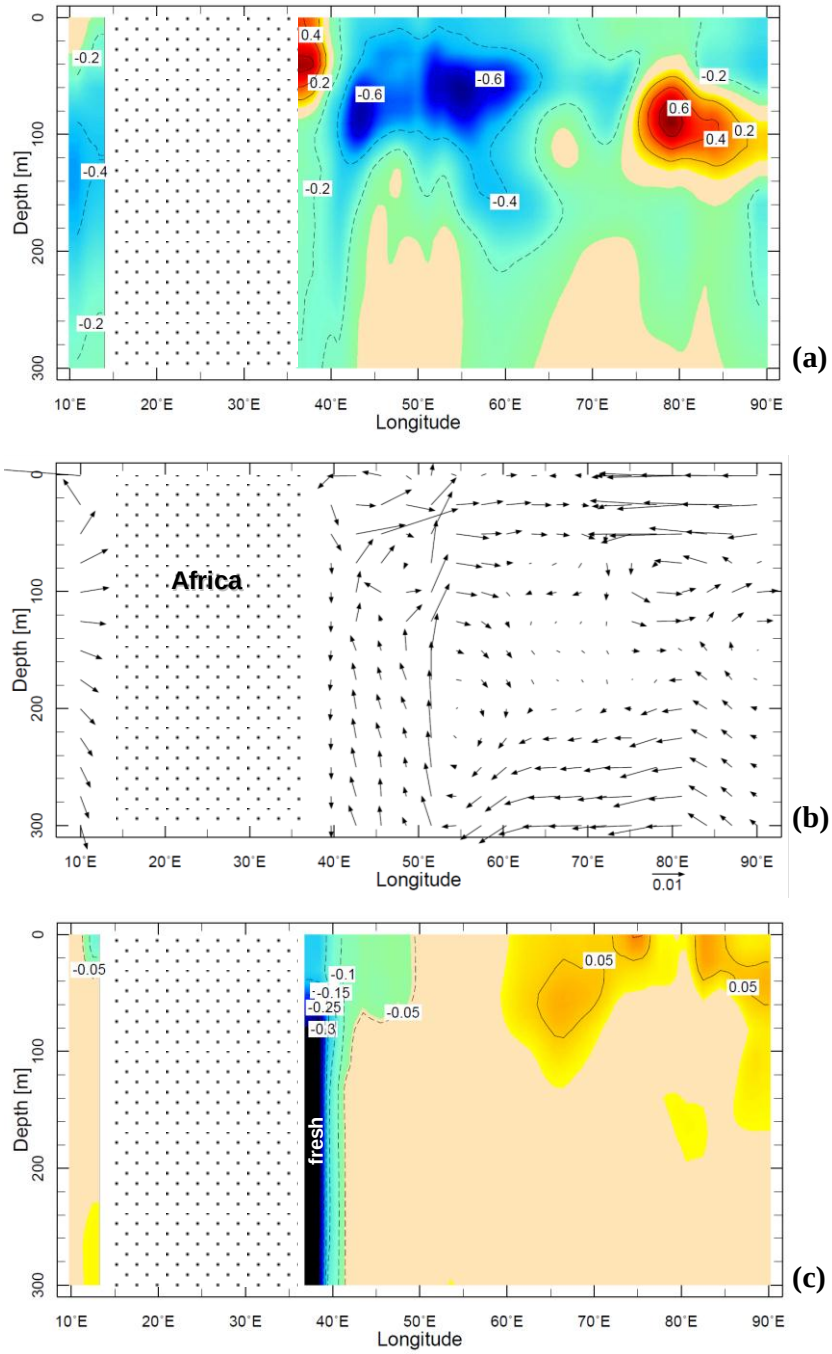

Figure 4. Composite high minus low (vegetation) difference of Jul-Oct sub-surface ocean (a) temperature, (b) zonal circulation and (c) salinity (ppt), in depth section averaged 10S-20N.

Ocean and warmer west Pacific Ocean similar to Rowell (2013), but elsewhere weak values are found. The ENSO (cold) signal is 'not ready' in the preceding year. The December to March sea level air pressure map is dominated by a global dipole of positive values over the Americas and negative values over Southeast Asia. This wave-one feature is consistent with the decadal dipole of White and Tourre (2003, 2007) that refers to an interaction of ENSO and south Indian Ocean Rossby wave (Jury and Huang, 2004). As a result of the high

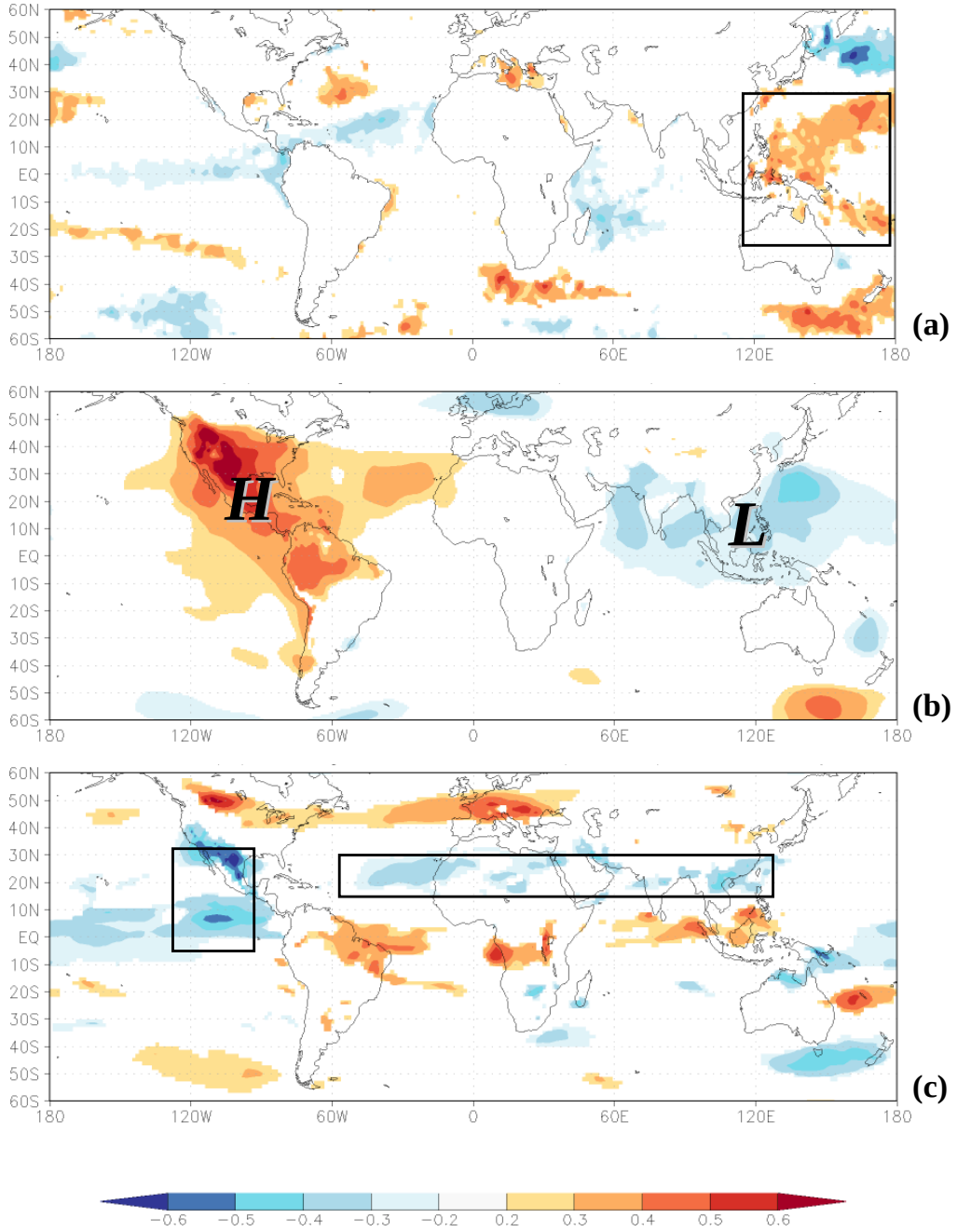

Figure 5. Correlation maps at December to March lead time in respect of July to October vegetation for (a) SST, (b) SLP, and (c) 850 hPa zonal wind. Predictors used in the multi-variate algorithm are identified with boxes. Insignificant correlations are shaded neutral.

pressure over the Americas, the zonal wind correlations are negative over the northeast Pacific. Elsewhere there is a band of negative correlation across North Africa and Southern China and an opposing band of positive zonal wind correlation near the equator from Brazil to the Maritime Continent. A positive correlation also exists across the north Atlantic mid-latitudes. These patterns for the preceding December to March are useful to extract key predictor time series and develop a multi-variate algorithm to forecast changes in July to October vegetation fraction, as a proxy for crop yield in Ethiopia. After back-ward stepwise regression and elimination of weaker predictors, a three parameter algorithm is formed that generates a 6-month lead forecast. The time series

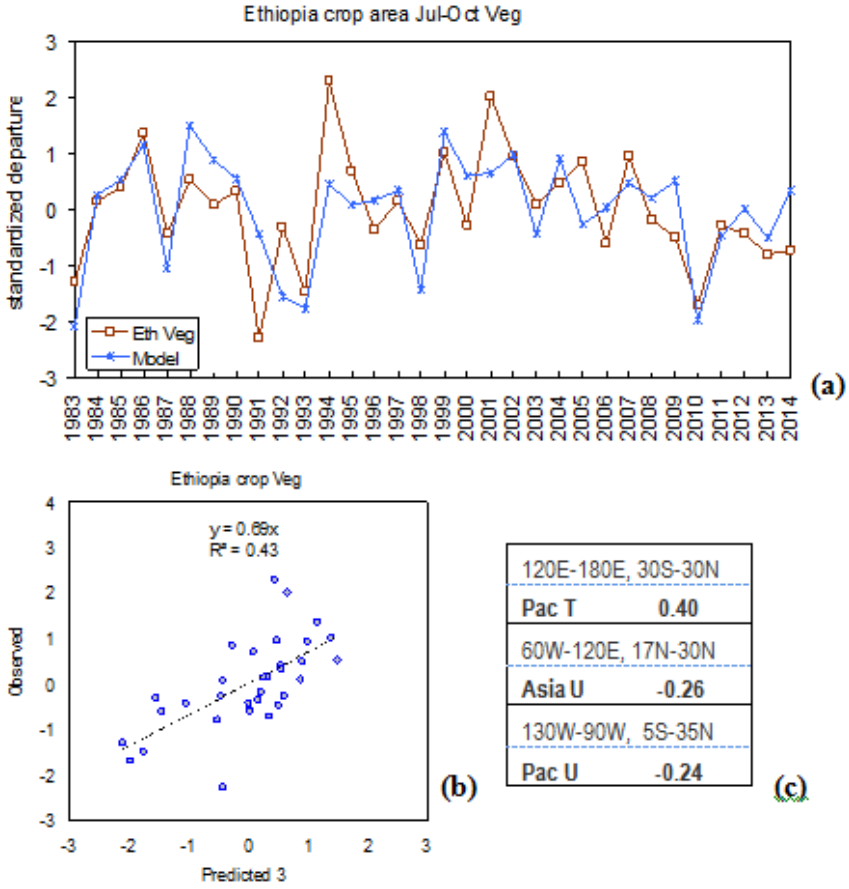

Figure 6. Observed and predicted Ethiopian highlands July to October vegetation as (a) time series and (b) scatterplot and fit. (c) Table of predictor domain and influence (bold).

and scatterplot comparisons are given in Figure 6a and b. The leading predictor is west Pacific SST (warm favourable), followed by Asia zonal winds and Pacific zonal winds (easterly favourable). The model fit (43%) is on the borderline of statistical significance, typical for northern summer climate. The tercile hit rate is 64% in the below category, with misses in 1991 and 2014, and 82% in the above category with weak performance in 1995 and 2005. The model predicts low vegetation fraction in 1983, 1993 and 2010, but under-predicts the high years of 1994 and 2001. The predictors apparently foretell of chances for a convective dipole between the east Indian Ocean and central Africa (Figure 2a).

Conclusions

The vegetation fraction over the Ethiopian highlands exhibits large seasonal and multi-annual variability in the period 1982 to 2014. Northern areas are more sensitive to rainfall due to the brevity of the wet season and proximity to arid zones. In comparison with parallel work using rainfall over the same place and era, our vegetation index exhibits markedly different teleconnections.

The regional climate influence was expressed in (high minus low vegetation) composites of rainfall, wind, humidity, sea temperatures, salinity and currents; and correlations at six-month lead-time. The key climatic driver of vegetation is the zonal overturning atmospheric circulation linking subsidence over the east Indian Ocean and ascent within an expanded African monsoon (Figure 3a and b). Certain features of this Walker Cell reflect Pacific ENSO interaction with the Indian Ocean Dipole (Figure 4a) which, during cold phase, induces an upwelling Rossby wave and cool sea temperatures, as outlined in White and Tourre (2007). It is odd that convection is suppressed over India during years of above normal vegetation in Ethiopia, as prior work has shown that an active Indian monsoon enhances the upper easterly jet and Nile River flow (Camberlin, 1997; Jury, 2011). Further study of this feature and its stability is needed.

Conflict of Interest

The authors have not declared any conflict of interest.

ACKNOWLEDGEMENTS

This study is part of a Rockefeller Foundation project with the Ethiopian Institute for Agricultural Research, Melkasa, conceived with help from F. Mequanint and G. Mamo. Web-based analyses were made using the IRI Climate Library, the KNMI Climate Explorer, and the NCEP ESRL-PSD composite mapping system.

REFERENCES

Adler RF, Huffman GJ, Chang A, Ferraro R, Ping-Ping X,John J, Bruno R, Udo S, Scott C, David B, Arnold G, Joel S, Philip A, Eric N (2003). The version 2 Global Precipitation Climatology Project (GPCP) monthly precipitation analysis (1979-Present). J. Hydrometeor 4:1147-1167.

Al-Bakri JT, Suleiman AS (2004). NDVI response to rainfall in different ecological zones in Jordan. Int. J. Remote Sens. 25:3897-3912.

Annamalai H, Xie S-P, McCreary JP, Murtugudde R (2005). Impact of Indian Ocean sea surface temperature on developing El Nino. J. Clim. 18:302-319.

Anyamba A, Eastman JR (1996). Interannual variability of NDVI over Africa and its relation to El Niño/Southern Oscillation. Int. J. Remote Sensing 17:2533-2548.

Anyamba A, Tucker CJ, Eastman JR (2001). NDVI anomaly patterns over Africa during the 1997/98 ENSO warm event. Int. J. Remote Sensing 22:1847-1859.

Anyamba A, Tucker CJ, Mahoney R (2002). From El Niño to La Niña: Vegetation response patterns over eastern and southern Africa during the 1997-1998 period. J. Clim. 15:3096-3103.

Bannari A, Morin D, Bonn F (1995). A review of vegetation indices. Remote Sensing Rev. 13:95-120

Behringer DW (2007). The Global Ocean Data Assimilation System (GODAS) at NCEP. Proc. 11th Symp. Integr. Obs. Assim. Systems, San Antonio, TX, Amer. Meteor. Soc. 3.3.

Budde ME, Tappan G, Rowland J, Lewis J, Tieszen LL (2004). Assessing land cover performance in Senegal, West Africa using 1-km integrated NDVI and local variance analysis. J. Arid Environ. 59:481-498.

Cane MA, Eshel G, Buckland RW (1994). Forecasting Zimbabwean maize yield using eastern equatorial Pacific sea-surface temperature. Nature 370:204-205.

Camberlin P (1997). Rainfall anomalies in the source region of the Nile and their connection with the Indian summer monsoon. J. Clim. 10:1380-1392.

Carleton AM (1998). Ocean-Atmosphere Interactions, in Encyclopedia of Environmental Analysis and Remediation. RA Meyers (ed), Wiley, New York. Pp. 3151-3188.

Cassel-Gintz MA, Lüdeke MKB, Petschel-Held G, Reusswig F, Pöchl M, Lammel G, Schellnhuber HJ (1997). Fuzzy logic based global assessment of marginality of agricultural land use. Clim. Res. Int. Clim. Ecosys. Human Soc. 8:135-150.

Chappell A, Seaquist JW, Eklundh L (2001). Improving the estimation of noise from NOAA AVHRR NDVI for Africa using geostatistics. Int. J. Remote Sensing 22:1067-1080.

Davenport ML, Nicholson SE (1993). On the relation between rainfall and the Normalized Difference Vegetation Index for diverse vegetation types in East Africa. Int. J. Remote Sens. 14:2369-2389.

Dee DP, Uppala SM, Simmons AJ, Berrisford P, Poli P, Kobayashi S, Andrae U, Balmaseda MA, Balsamo G, Bauer P, Bechtold P, Beljaars ACM, van de Berg L, Bidlot J, Bormann N, Delsol C, Dragani R, Fuentes M, Geer AJ, Haimberger L, Healy SB, Hersbach H, Hólm EV, Isaksen L, Kållberg P, Köhler M, Matricardi M, McNally AP, Monge-Sanz BM, Morcrette JJ, Park BK, Peubey C, de Rosnay P, Tavolato C, Thépaut JN, Vitart F (2011). The ERA-Interim reanalysis: configuration and performance of the data assimilation system. Q. J. Royal Met. Soc. 137:553-597.

Eklundh L (1998). Estimating relations between AVHRR NDVI and rainfall in East Africa at 10-day and monthly time scales. Int. J. Remote Sens. 19:563-568.

Eklundh L, Sjöström M (2005). Analysing vegetation changes in the Sahel using sensor data from Landsat and NOAA. in: Proc Intl Sym Remote Sensing Environment, St. Petersburg FL.

Hastenrath S (2000) Zonal circulations over the equatorial Indian Ocean. J. Clim. 13:2746-2756.

Herrmann SM, Anyamba A, Tucker CJ (2005). Exploring relationship between rainfall and vegetation dynamics in the Sahel using coarse resolution satellite data. In: Proc Int. Symp. Remote Sens. Environ. June 20-24, St. Petersburg.

Huete A, Didan K, Miura T, Rodriguez E, Gao X, Ferreira L (2002). Overview of the radiometric and biophysical performance of the MODIS vegetation indices, Remote Sens. Environ. 83:195-213.

Jury MR, Huang B (2004) The Rossby wave as a key mechanism of Indian Ocean climate variability. Deep Sea Res. 51:2123-2136.

Jury MR (2011). Climatic factors modulating Nile River flow, in Nile River Basin part IV, ed. AM Melesse, Springer, pp. 267-280.

Jury MR (2013). Ethiopian highlands crop-climate prediction 1979-2009. J. Appl. Meteorol. Climatol. 52:1116-1126.

Kanamitsu Ma, Wesley E, Jack W, Shi-Keng Y, Hnilo JJ, Fiorino M, Potter GL (2002) NCEP-DOE AMIP-II Reanalysis (R-2). Bull. Amer. Meteor. Soc. 83:1631-1643.

Kawabata A, Ichi K, Yamaguchi Y (2001). Global monitoring of interannual changes in vegetation activities using NDVI and its relationships to temperature and precipitation. Int. J. Remote Sens. 22:1377-1382.

Kennedy JJ, Rayner NA, Smith RO, Saunby M, Parker DE (2011). Reassessing biases and other uncertainties in sea-surface temperature observations since 1850 part 1: measurement and sampling errors. J. Geophys. Res. P. 116.

Kogan FN (1998). A typical pattern of vegetation conditions in southern Africa during El Niño years detected from AVHRR data using three-channel numerical index. Int. J. Remote Sens. 19:3689-3695.

Kug JS, An SI, Jin FF, Kang LS (2005). Preconditions for El Nino and La Nina onset and their relation to the Indian Ocean. Geophys. Res. Lett. 32:L05706.

Kug JS, Li T, An SI, Kang LS, Luo JJ, Masson S, Yamagata T (2006). Role of the ENSO–Indian Ocean coupling in ENSO variability in a coupled GCM. Geophys. Res. Lett. 33:L09710.

Lewis J E, Rowland J, Nadeau A (1998). Estimating maize production in Kenya using NDVI: some statistical considerations. Int. J. Remote Sens. 19:2609-2617.

Li J, Lewis J, Rowland J, Tappan G, Tieszen LL (2004). Evaluation of land performance in Senegal using multi-temporal NDVI and rainfall series. J. Arid Environ. 59:463-480.

Luo JJ, Zhang R, Behera SK, Masumoto Y, Jin FF, Lukas R, Yamagata T (2010). Interaction between El Niño and extreme Indian Ocean Dipole. J. Clim. 23:726-742.

Maselli F, Romanelli S, Bottai L, Maracchi G (2000). Processing of GAC NDVI data for yield forecasting in the Sahelian region. Int. J. Remote Sensing 21: 3509-3523.

Mennis J (2001) Exploring relationships between ENSO and vegetation vigour in the southeast USA using AVHRR data. Int. J. Remote Sens. 22:3077–3092.

Myneni RB, Los SO, Tucker CJ (1996). Satellite-based identification of linked vegetation index and sea surface temperature anomaly areas from 1982–1990 for Africa, Australia, and South America. Geophys. Res. Lett. 23:729-732.

Philippon N, Martiny N, Camberlin P, Hoffman MT, Gond V (2014). Timing and patterns of the ENSO Signal in Africa over the last 30 years: insights from Normalized Difference Vegetation Index data. J. Climate 27:2509–2532.

Plisnier PD, Serneels S, Lambin EF (2000). Impact of ENSO on East African ecosystems: a multivariate analysis based on climate and remote sensing data, Glob. Ecol. Biogeogr. 9:481-497.
Reed BC, Brown JF, VanDerZee D, Loveland TR, Merchant JW, Ohlen DO (1994). Measuring phenological variability from satellite imagery. J. Vegetation Sci. 5:703-714.
Richard Y, Poccard I (1998). A statistical study of NDVI sensitivity to seasonal and interannual rainfall variations in Southern Africa. Int. J. Remote Sens. 19:2907-2920.
Ropelewski CF, Halpert MS (1987). Global and regional scale precipitation patterns associated with El Niño/Southern Oscillation. Mon Weather Rev. 115:1606-1626.
Rowell DP (2013). Simulating SST teleconnections to Africa: what is the state of the art? J. Clim. 26:5397-5418.
Saji NH, Goswami BN, Vinayachandran PN, Yamagata T (1999) A dipole mode in the tropical Indian Ocean. Nature 401:360-363.
Tucker CJ (1979) Red and photographic infrared linear combinations for monitoring vegetation. Remote Sens. Environ. 8:127-150.
Tuckera CJ, Jorge EP, Molly EB, Daniel AS, Edwin WP, Robert M, Eric FV, El Saleousa N (2005). An extended AVHRR 8-km NDVI data set compatible with MODIS and SPOT vegetation NDVI data. Int. J. Remote Sensing 26:4485-5598.
Vanacker V, Linderman M, Lupo F, Flasse S, Lambin E (2005). Impact of short-term rainfall fluctuation on interannual land cover change in sub-saharan Africa. Glob. Ecol. Biogeogr. 14:123-135.
Verdin J, Funk C, Klaver R, Roberts D (1999) Exploring the correlation between Southern Africa NDVI and Pacific sea surface temperature: results for the 1998 maize growing season. Int. J. Remote Sens. 20:2117-2124.
White MA, Thomton PE, Running SW (1997). A continental phenology model for monitoring vegetation responses to interannual climatic variability. Glob. Biogeochem. Cycles 11:217-234.
White WB, Tourre YM (2003). Global SST/SLP waves during the 20th century. Geophys. Res. Lett. 30:53-57.
White WB, Tourre YM (2007). A delayed action oscillator shared by the ENSO and QDO in the Indian Ocean. J. Oceanogr. 63:223-241.
Young SS, Harris R (2005). Changing patterns of global-scale vegetation photosynthesis, 1982–1999. Int. J. Remote Sens. 26:4537-4563.
Zhang X, Friedl MA, Schaaf CB, Strahler AH (2005). Monitoring the response of vegetation phenology to precipitation in Africa by coupling MODIS and TRMM instruments. J. Geophys. Res. P. 110.

academicJournals

Related Journals Published by Academic Journals

- International NGO Journal
- International Journal of Peace and Development Studies